Electromagnetic Braking System

Tufts Department of Mechanical Engineering
ME70 Final Report

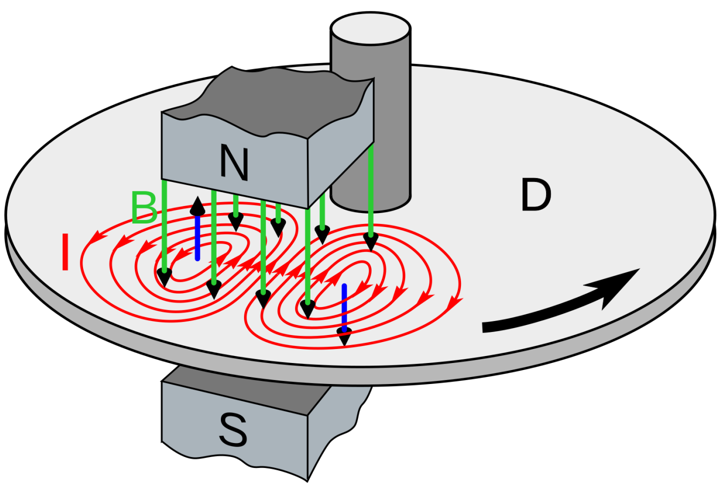

David Zhang, Maxwell Battles, Tue Nguyen, Odin Doolittle, Madeline Fabela, Leslie Jaramillo Martinez

05/06/2021

Executive Summary

Through the usage of eddy-current braking systems, demands for braking technologies that are independent of friction have been fulfilled. When an electrically-conductive wheel crosses a region of changing electromagnetic field, the moving body begins to decelerate with a smooth and quiet transition. Traditional braking systems rely upon the friction produced between the wheel and a brake pad, but with high-momentum loads, this becomes inefficient. Unlike these frictional braking systems, eddy-current brakes operate through the current that is induced by the electromagnet into the wheel. This current produces an opposing magnetic field. As the field causes a decrease in the speed of the wheels, the mechanical energy present transforms into heat energy, which negatively impacts the efficiency of the brake. In this experiment, we study the effects of eddy currents on the temperature and deceleration of three disks. Initially, a model of the electromagnetic brake used in a high-speed railway was used; however, permanent magnets were used instead for data collection. Three aluminum disks of the same inertia–but with holes of varying sizes cut out–were tested for deceleration and temperature change. A testbed was built to hold the motor, disk, and encoder in place. Each disk was run five times and was introduced to magnets after it had reached a stable speed. The results indicated little to disk temperature change occurred and that increasing the diameter of the disk's holes reduced the braking efficiency of the system.

Table of Contents

Introduction

As part of any braking system for moving vehicles, the efficiency of brakes determines how quickly a moving object can be stopped to avoid long deceleration distance and ensure the passenger's safety in case of an emergency. The most commonly used braking mechanism, found in cars and bikes, utilizes the friction force caused by a pair of pads squeezing onto the disk to slow the shaft rotation. However, for subways and roller coasters, a different braking mechanism called eddy current brakes are utilized to slow down heavy-weight and high-speed vehicles effectively. The theory behind this braking system is as follows. Through Faraday's law of induction, the changing magnetic flux of the electromagnets creates an electric field and current onto the conductive, non-ferrous disk. This induced current found on the brake disk is called Eddy Current. Then, with Lenz's Law, the induced Eddy Current will generate a magnetic field on the non-ferrous disk. Since the motor is still constantly powering the disk to rotate at a constant speed, an opposing electromotive force will be created and slow down the braking disk, with heat being generated on the disk as a by-product. Most importantly, the braking efficiency drops as the disk brake's temperature increases. Prior research has been conducted on the best material for the braking disk[1] and the optimal arrangement of the electromagnets[2], but there is a lack of literature on how the disk's geometry can be utilized to reduce the effects of an increase in temperature while still decelerating the disk swiftly. Our group set out to build a physical model of the electromagnetic brake used in a high-speed railway. Three aluminum disks of the same inertia and varying eddy currents were tested for deceleration and temperature change. One disk, the control, lacked holes. The other two had holes of different sizes cut out from them. A testbed was built to hold the motor, disk, and encoder in place. Each disk was run five times and was introduced to magnets after it had reached a stable speed. We hypothesize that the larger holes will allow for greater heat dissipation to occur in the disk, but at the cost of how efficient the disk is at decelerating. We aim to provide the testing results of eddy current brakes to the general public, as we believe it is very important for the end-users to be aware and validate the safety of these under-explored braking systems.

<u>Methods</u>

I: Setup and Data Collection

A physical setup was built to control and measure the rotation of an aluminum disk for its non-ferrous property. The disk was driven by a NEMA 23 stepper motor which was controlled by an Arduino Uno and a digital stepper driver DM542T. This actuation module was mounted on a base that was parallel to the floor with the shaft of the motor normal to the base pointing towards the ceiling. The shaft of the motor was not long enough to hold a rotary encoder and the aluminum disk, so it was designed to directly drive a large 20cm diameter wheel and transmit this motion to a small 4 cm diameter wheel using a belt. The small wheel was concentric to a long 10mm diameter shaft, the encoder, and the disk. The small wheel and the disk were fixed on the shaft using collars to allow it to be driven, while the encoder was mounted on a top cover and only allowed its inner part to be fixed to the shaft. The encoder was wired to a NI myRIO which could visualize data through LabVIEW. Bearings were applied to the connections between the long shaft and the top cover and the base to reduce friction during rotation.

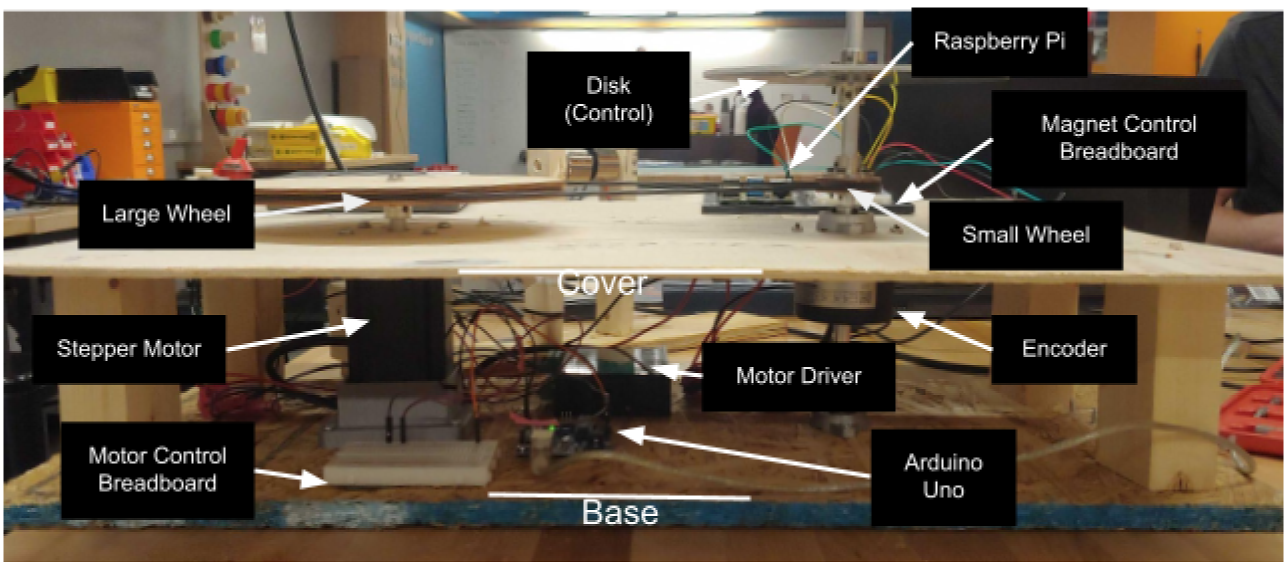

Figure 1: Side view of physical setup without electromagnets. The space between the cover and base contains most of the control units while motion happens above the cover.

On the end of the aluminum disk, a stand was placed to hold two electromagnets in place. The stand was designed to leave a gap in between the magnets so the disk would fit. A Raspberry Pi was used to control the magnitude and polarity of the electromagnets. In order to test our hypothesis, three disks with no holes (control), small holes, and large holes were examined under the magnetic field while their moment of inertia remained identical.

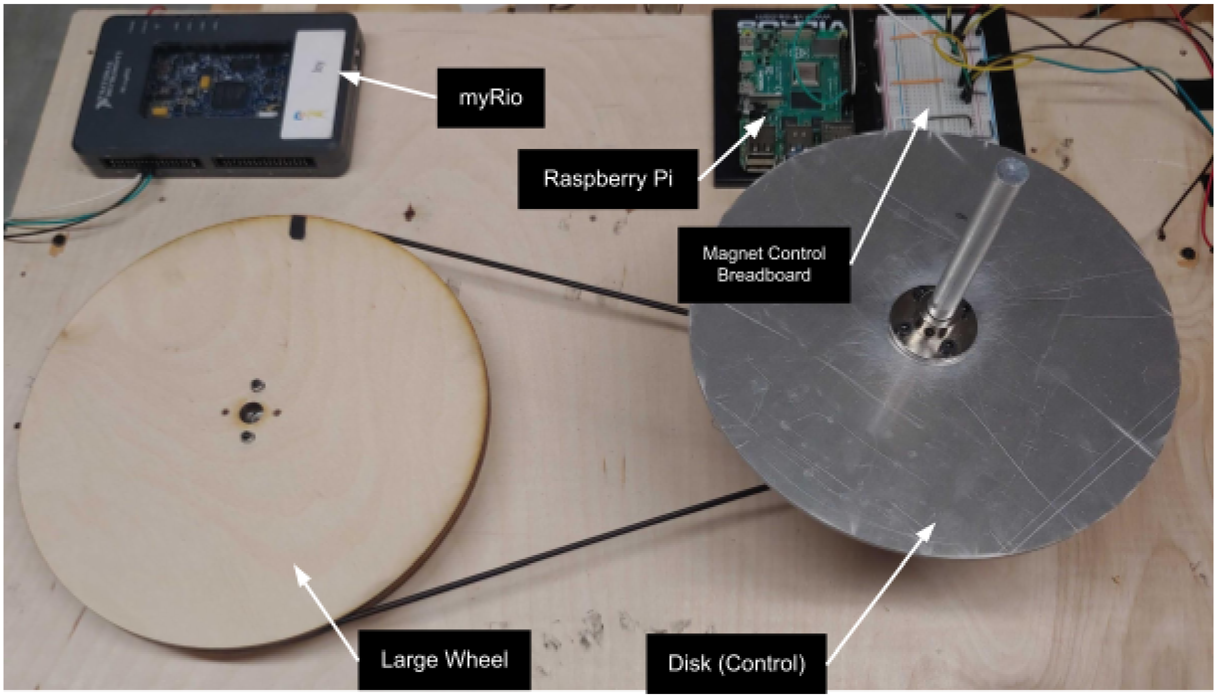

Figure 2: Top view of physical setup without electromagnets. The large wheel (D=20cm) drives a small wheel (d=4cm) underneath the disk. The small wheel and the disk are connected to the shaft so they will rotate at the same time.

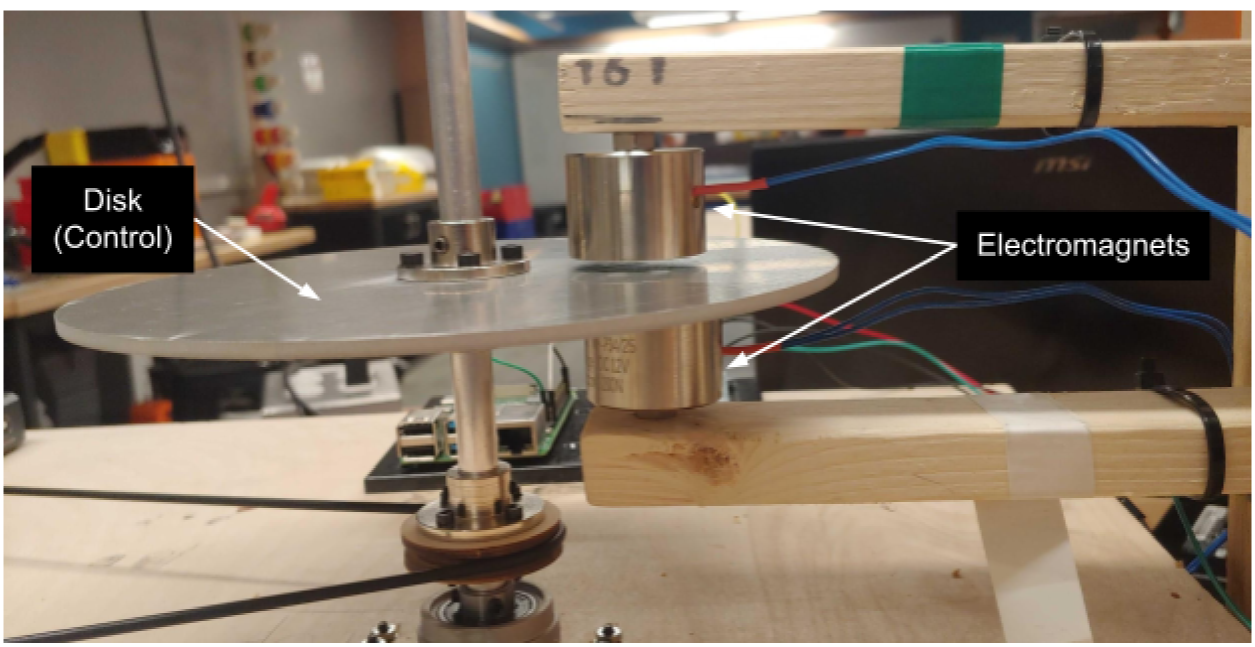

Figure 3a: Close-up view of electromagnets mounted on physical setup. The magnets are controlled by the Raspberry Pi. Their polarity should be opposite to induce an eddy current on the disk.

II: Processing

The experiment would start with powering the motor driver with 24V and 1.91A and run the code uploaded to the Arduino Uno. Then electromagnets were activated by the Raspberry Pi. Meanwhile, an infrared gun was pointed toward the disk to observe any trail of temperature change on the disk caused by the magnets. However, we failed to see any response by the disks to the applied electromagnets, and instead used permanent, Neodymium magnets (See *Figure 3b*). We believe that since our electromagnets were fed DC instead of AC current, they could not induce the type of magnetic field required for eddy-current creation.

The rotation data was collected, transferred to LabVIEW through myRIO, and processed in LabVIEW for calibration, calculation of angular displacement and velocity, and moving average. The processed data was visualized in real-time on the LabVIEW plots. After the collection finished, the data was extracted to Excel and processed again in MATLAB for filtering and statistical analysis. Each disk ran for five trials. The same process was also done after replacing electromagnets with permanent magnets.

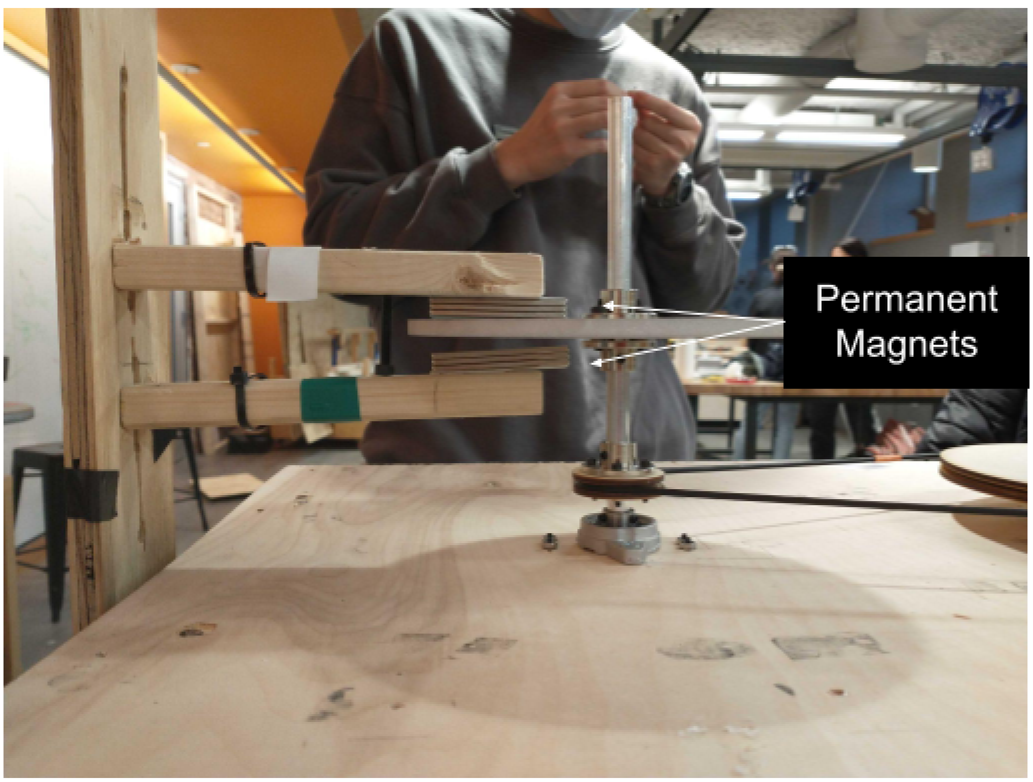

Figure 3b: Close-up view of permanent magnets mounted on the physical setup. We slid this into position after the disk reached its steady-state speed.

Results

The primary method of data collection granted us a look at how the speed of the disk at each sample collected through the encoder with 10 ms between samples. Results were processed to produce three categories of observable and usable data. The first category is raw encoder data. The five trials are shown separately for each disk, and the point where braking begins was then marked for further processing. After using a Butterworth filter with a 2nd order filter and .02 normalized cutoff frequency and filtfilt() function, the now processed data was cut down to start at the point the braking was applied and ended after a specified number of trials for each disk. Finally, this data was broken into two categories, a deceleration period where the braking was applied and velocity decreased and a steady-state period where the force of the motor equaled the force of the braking force. This data is displayed with all 15 trials on the same plot and distinguished by color.

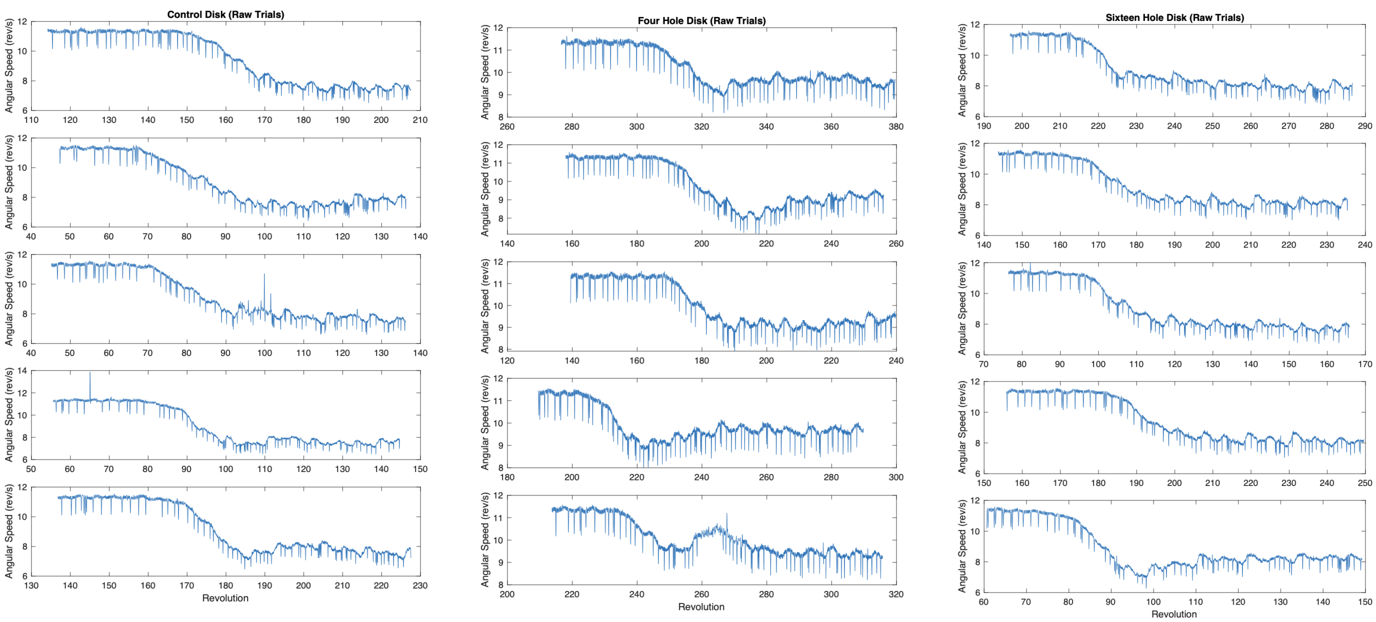

Figure 4: Plots of control, four-hole, and sixteen-hole disk velocity per sample for each of the five trials.

The plots show the raw, unfiltered angular speed from the start of data recording to the end for each of the five trials for the three disks. Notably, the point of braking was not consistent between trials which warranted manual selection of braking point for further processing.

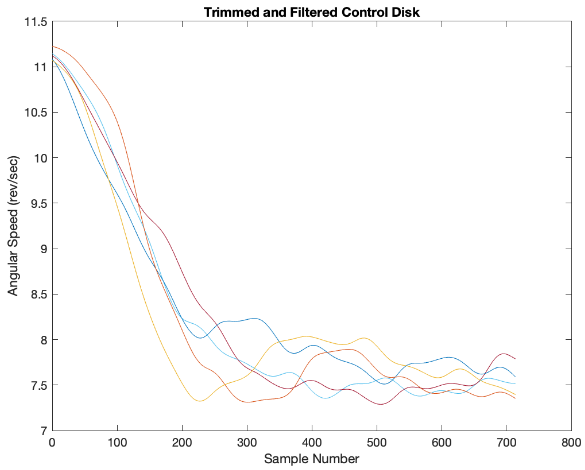

Figure 5: Filtered velocity of the control disk.

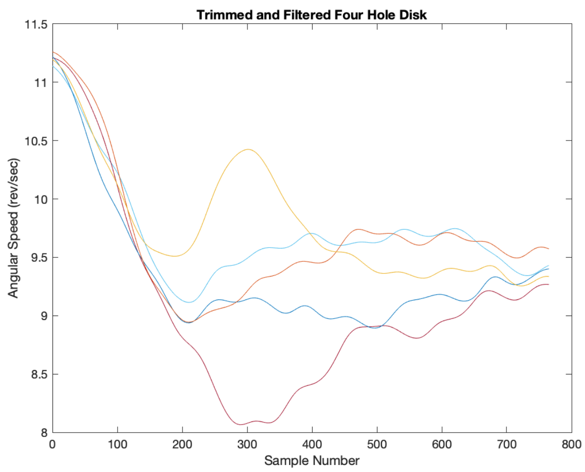

Figure 6: Filtered velocity of the 4-hole disk.

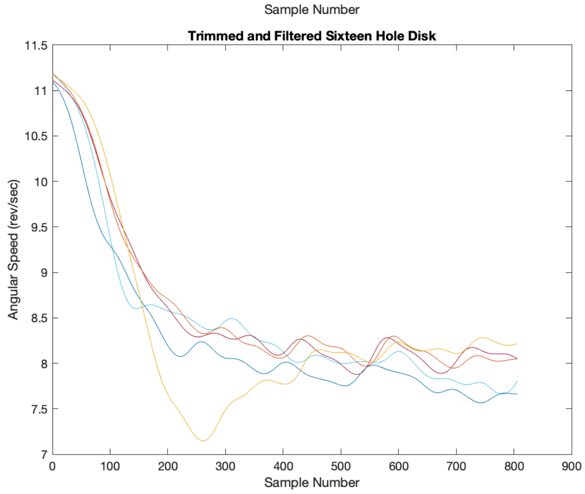

Figure 7: Filtered velocity of the 16-hole disk.

These plots show the angular speed filtered from the point of breaking until a specified encoder count. The goal was to optimize the number of points observable while constraining the data to the same length. Initial observations indicate a higher steady-state error for the four-hole disk. Further processing is required for comparison.

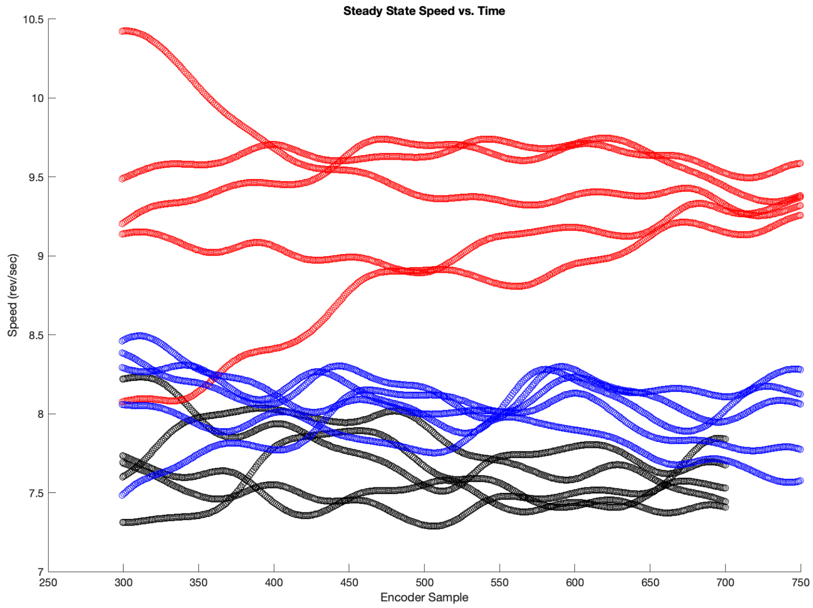

Figure 8: Steady-State Speed of Each Trial

This figure shows each of the 15 trials during the steady-state portion after braking was applied. The black is the control disk, the blue is for the sixteen-hole disk, and the red is the four-hole disk. Initial review shows that the control disk had the lowest steady-state speed and the four-hole disk had a significantly higher steady-state speed than the other two disks.

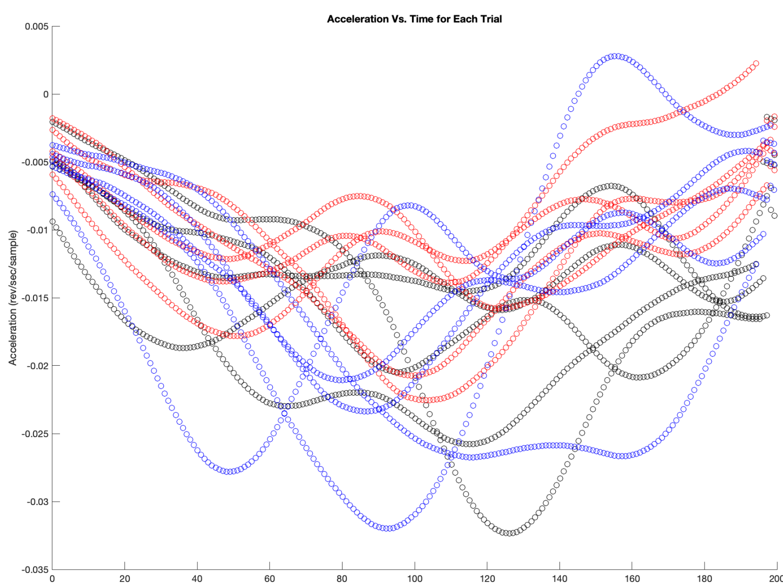

Figure 9: Acceleration During Initial Braking for Each Trial

This figure shows the differentiated speed or deceleration during the initial braking period for each disk. The black is the control disk, the blue is the sixteen-hole disk, and the red is the four-hole disk. More processing is required for meaningful interpretation of this graph.

Sample	Steady State p-value	Acceleration p-value
Control and Four Holes	1.2372e-05	0.0073
Control and Sixteen Holes	0.0014	0.5791
Four Holes and Sixteen Holes	7.1734e-05	0.0205

Table 1: Statistical analysis between each test.

This table shows the p-value between disks using the mean steady-state value and mean acceleration value of each trial. The p-values are generally quite small with the exception of the acceleration p-value between the control disk and sixteen-hole disk.

	Trial 1 Mean	Trial 2 Mean	Trial 3 Mean	Trial 4 Mean	Trial 5 Mean
Control Steady State (rev/s)	7.506	7.500	7.793	7.552	7.793
Sixteen Hole Steady State (rev/s)	8.046	8.117	7.848	8.140	8.016
Four Hole Steady State (rev/s)	9.609	8.772	9.111	9.565	9.555
Control Deceleration (rev/s/sample)	-0.0146	-0.0119	-0.0143	-0.0156	-0.0178
Sixteen Hole Deceleration (rev/s/sample)	-0.0131	-0.0126	-0.0145	-0.0124	-0.0176
Four Hole Deceleration (rev/s/sample)	-0.0101	-0.0120	-0.0114	-0.0115	-0.008

Table 2: Comparison of each trial and disk's velocity and rate of deceleration.

This table displays the mean value for each trial of each disk for the filtered stages of steady-state and deceleration. The steady-state velocity is displayed in revolutions/second and the acceleration is in revolutions/second/sample since the change is between 10ms samples.

In summary, the results highlight a difference between disk behavior during the acceleration phase and the steady-state phase. While not initially obvious in *Figure 4* which compares the raw data, a filtration and shift reveal early signs of distinction between disks in *Figure 5,* especially for the speed of steady-state disks. Further separation of the acceleration and steady-state phases allows a clear distinction of steady-state velocities. The control disk is slowed down the most, the sixteen-hole disk is slowed slightly less, and the four-hole disk is slowed significantly less. It is still difficult to graphically determine the difference between trials for the deceleration phase visually. This warrants statistical testing, which affirms beliefs of statistical distinction between the steady-state velocities of all three disks with p-values less than .05. The paired t-test also offers a statistically significant difference between acceleration means for the control with a four-hole pair and four-hole with sixteen-hole pair. It does not show a significant difference between the acceleration means for the control with sixteen hole pair. A comparison of means of the key data for each trial for the acceleration and steady-state phases is also helpful to examine and confirm our prior takeaways from the t-tests and graphics.

Discussion

There was an expectation for a change in temperature when the experiment was in its beginning stages. It was inferred that the mechanical energy of the motor had to be transformed into heat energy once the electromagnetic field forced the braking disks to stop rotating. As seen in *Figure 4* and *Table 2* across the trials, the braking disks decreased from 11.2 rev/sec to anywhere between 7.5 and 9.8 rev/sec in a matter of seconds. As soon as the permanent magnets were placed to surround the disk, there was a decrease in angular speed. Visually, it was a significant change in speed and led us to believe that there would be at least some increase in temperature. However, looking at the data, the drop in angular velocity was not drastic, though it was fast. Additionally, as the disk was spinning, it was cooling itself and the Fluke IR camera is meant to show longstanding and drastic changes in temperature rather than small incremental ones. Therefore, the results displayed in Appendix B reflect a rather static temperature throughout every trial.

Looking at the t-test results in *Table 1*, it can be concluded that in terms of design recommendations for the braking system, steady-state p-values reflect a comparison between the control and 4-hole disks, the control, and 16-hole disks, and the 4-hole and 16-hole disks can be done confidently. However, the p-values for acceleration reveal it would be wise to only make design recommendations comparing the control and 4-hole disk, as well as the 4-hole and the 16-hole disk. With this as a basis for the analysis, *Table 2* shows that the steady-state velocity of the control disk was the lowest, making the control disk braking system the most efficient in terms of its ability to decrease speed. Furthermore, the control disk system shows to have the highest rate of change in speed when compared to the 4-hole system. Meanwhile, the 16-hole disk system had a higher deceleration when compared to the 4-hole system. With these two criteria, decrease in speed and the rate of the change in speed, it is proven that the control disk system is the best overall and the 4-hole disk was the worst. This leads to a design recommendation to avoid holes that directly affect the eddy currents of the magnetic field since the holes failed to significantly show an increased rate of convection between the disk and atmosphere.

Impact and Conclusion

This experiment successfully studied the effect of eddy currents on the braking efficiency of three disks. As predicted, the disk with the most uniformity and thus uninterrupted eddy currents was the most efficient in decelerating. However, there are a variety of limitations in the experiment that make it difficult to hypothesize which disk design would be applicable for large-scale wheels. High-speed railways can reach a speed of up to 155 mph, which was not a speed our motor could achieve. In real-world applications, the magnetic field is introduced after the conductive wheels have reached a high and constant speed and thus are much stronger than the magnets used in this experiment. Additional limitations were based on the undersupply of material.

Overall, the differences in torque, disk size, electromagnetic field strength, and motor speed between the experimental disk and industry electromagnetic braking system limited our findings to the study of how the system worked and what the factors of influence were. In the future, it would be ideal to model a larger disk and a more automated testbed in which each trial is run for longer, the magnets are introduced at the same time, and the start and end times are the same. Although it was not suitable to make design suggestions for industry electromagnetic braking systems, the experiment allowed for an understanding and application of eddy-current brakes on a smaller scale.

Bibliography

[1] Baharom, M. Z., Nuawi, M. Z., Priyandoko, G., & Haris, S. M. (2009). Electromagnetic Braking System Using Eddy Current for Brake Disc of Al6061 and Al7075. *International Review of Mechanical Engineering (I.RE.M.E.)*, *20*(10). Retrieved from https://www.researchgate.net/profile/Gigih-Priyandoko/publication/258682929_Eddy_current_braking_experiment_using_brake_disc_from_aluminium_series_of_A16061_and_A17075/links/5488f45f0cf268d28f090184/Eddy-current-braking-experiment-using-brake-disc-from-aluminium-series-of-A16061-and-A17075.pdf.

[2] Hollowell, T. C., Kahl, J. T., Stanczak, M. D., & Wang, Y. (n.d.). (tech.). *Eddy Current Brake Design for Operation with Extreme Back-drivable Eddy Current Motor*. Ann Arbor, MI: UNIVERSITY OF MICHIGAN LIBRARY.

Appendix A: Motor Control and Real-time Encoder Program

We wrote the following code to provide a PWM signal to the motor driver.

```
//ME070 Project -- code for the motor

// Define pins
int driverPUL = 7;    // PUL- pin

// Define PWM width and initial direction
int pd = 300;       // Pulse Delay period, controls speed of motor--longer period, slower motor

void setup() {
  pinMode (driverPUL, OUTPUT);
}

// Run pulse HIGH and LOW once each to create a 50% duty cycle (percentage recommended by the motor driver)
void loop() {
    digitalWrite(driverPUL,HIGH);
    delayMicroseconds(pd);
    digitalWrite(driverPUL,LOW);
    delayMicroseconds(pd);
}
```

We made the following LabVIEW block diagram and front panel to interface with the myRio "Joy" with the built-in encoder module to gather real-time data of the brake disk. Raw encoder counts were converted to revolution counts. From there, those values were differentiated via the DiscreteDerive.vi sub-module to get raw velocity signals. Since this signal is relatively noisy, we have also implemented a moving-average filter of 100 samples to smoothen the signal.

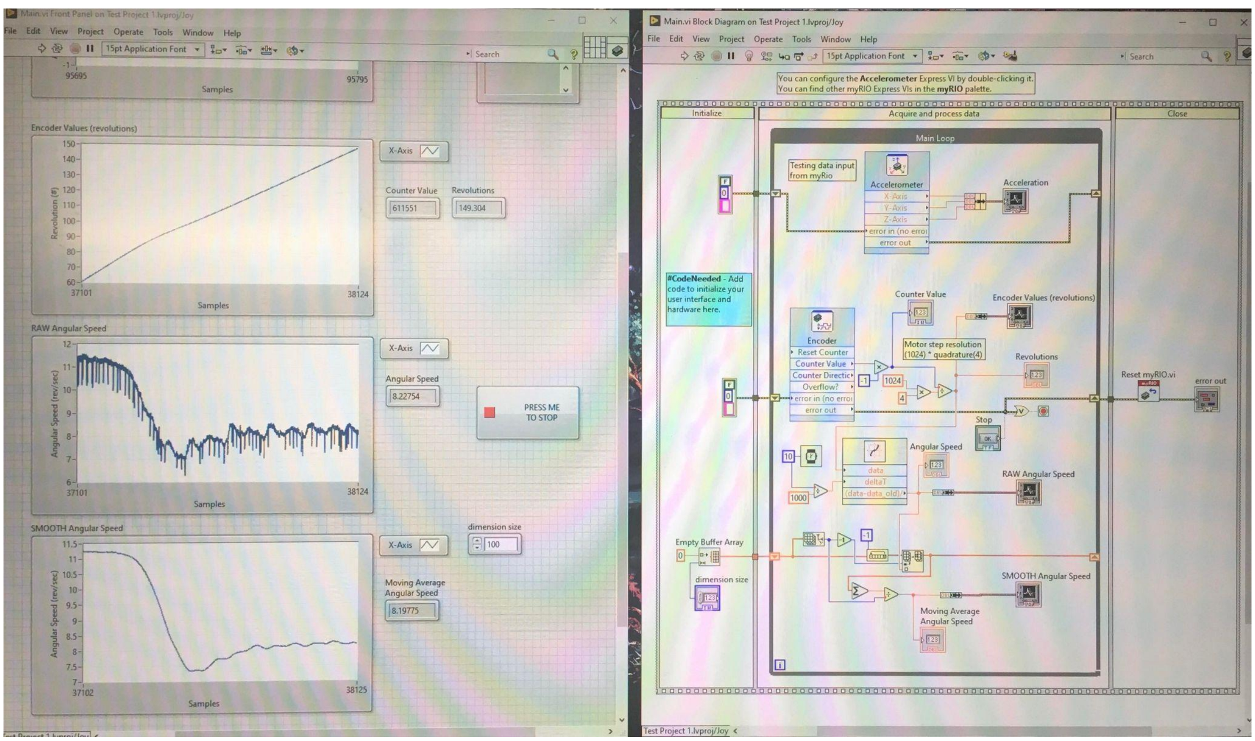

Appendix B: Thermal Images

For each of the five trials of each disk, we took thermal images before and–approximately 15 to 20 seconds–after the magnets were applied to the disk. This was done using the Fluke IR camera from Bray Lab.

Control Disk (No Holes)

Trial	Before Magnets	After Magnets
1	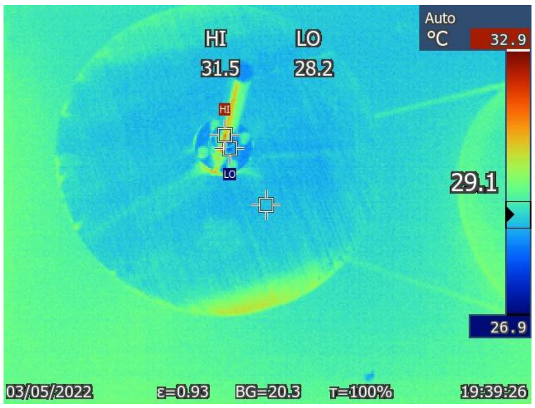	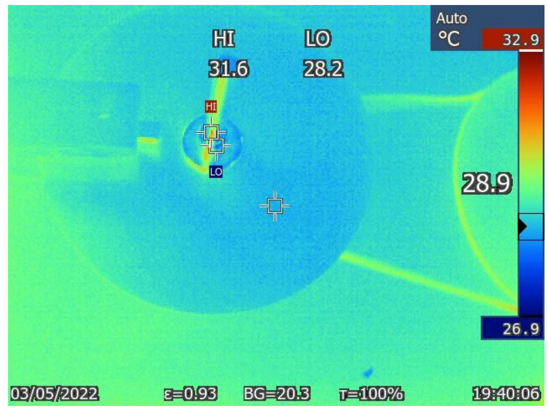
2	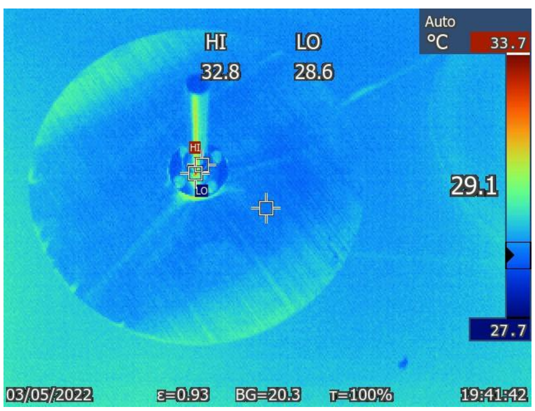	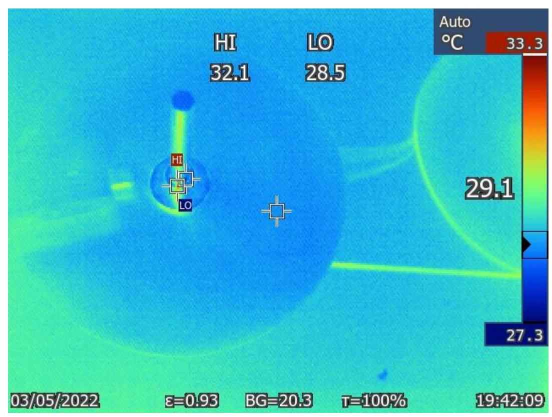
3	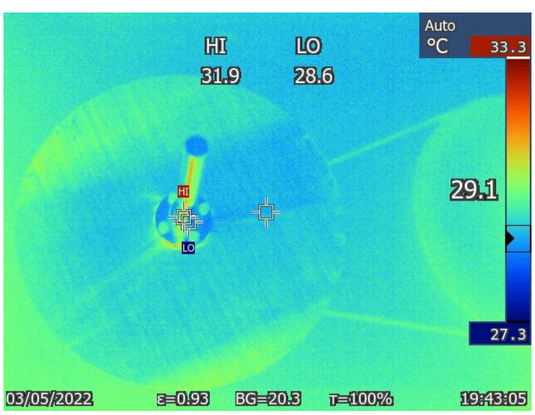	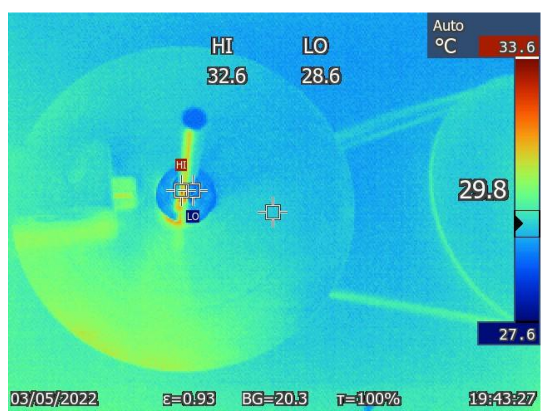

<table>
<tr><td>4</td><td>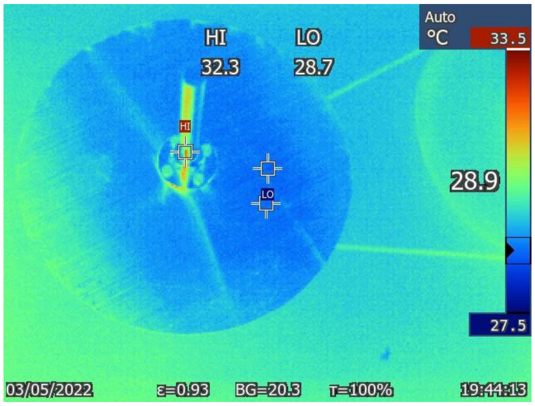
</td><td>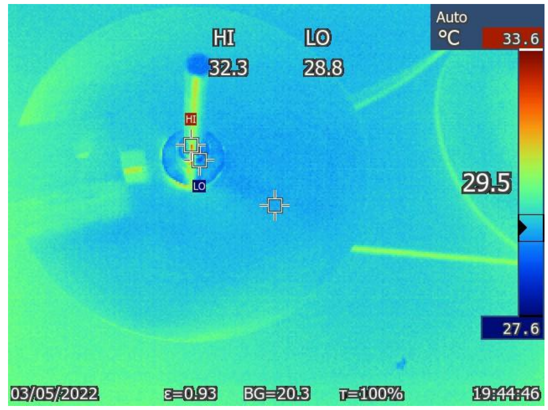
</td></tr>
<tr><td>5</td><td>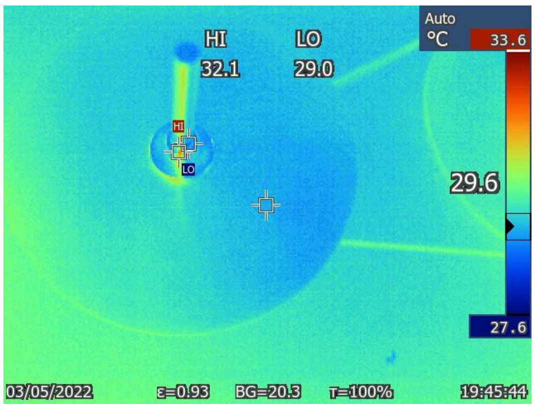
</td><td>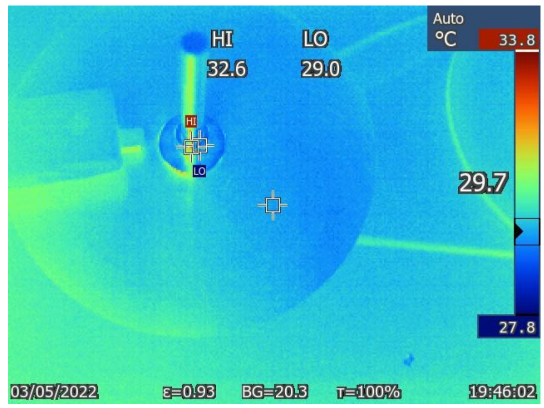
</td></tr>
</table>

4-Hole Disk

<table>
<tr><th>Trial</th><th>Before Magnets</th><th>After Magnets</th></tr>
<tr><td>1</td><td>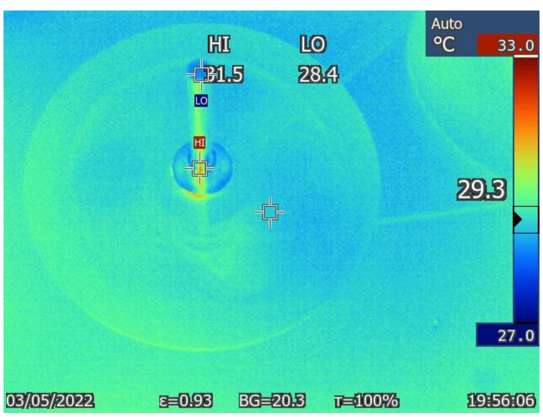
</td><td>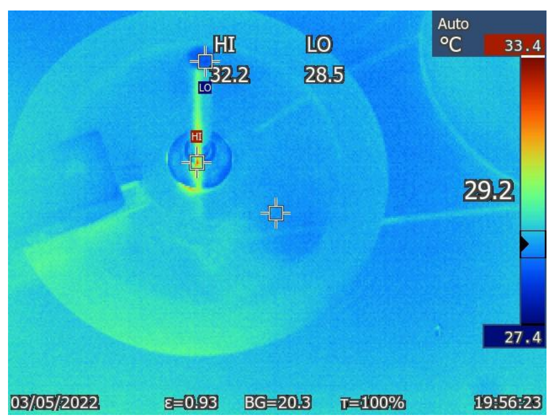
</td></tr>
</table>

<table>
<tr><td>2</td><td>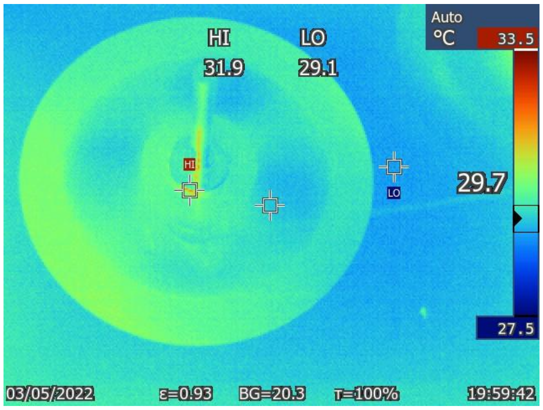
</td><td>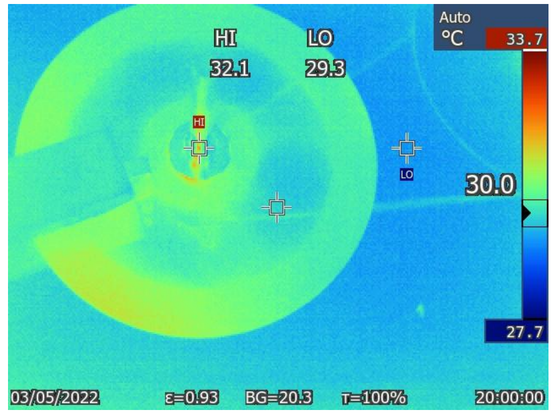
</td></tr>
<tr><td>3</td><td>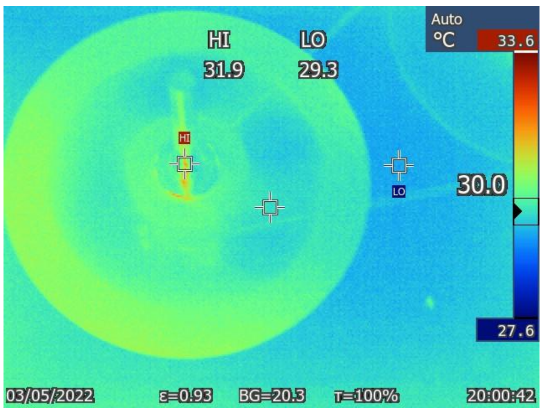
</td><td>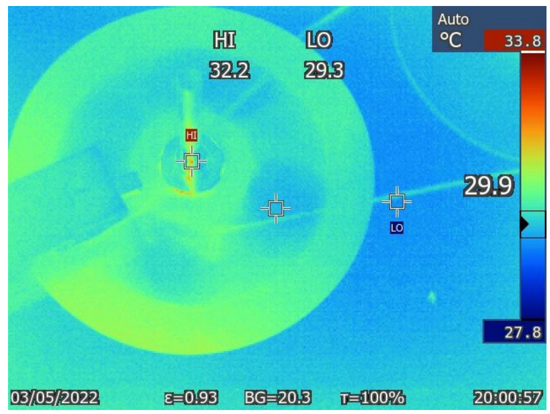
</td></tr>
<tr><td>4</td><td>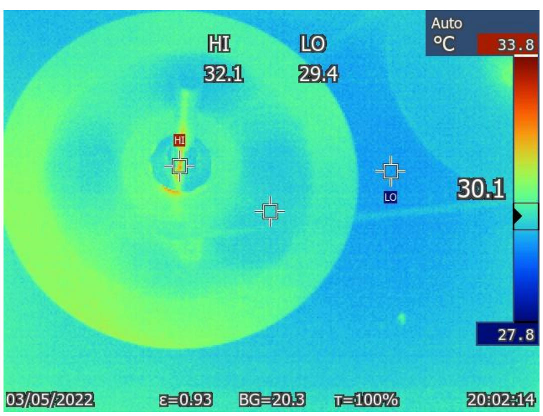
</td><td>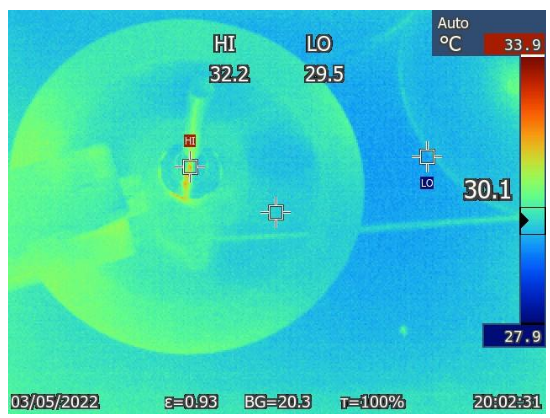
</td></tr>
</table>

5	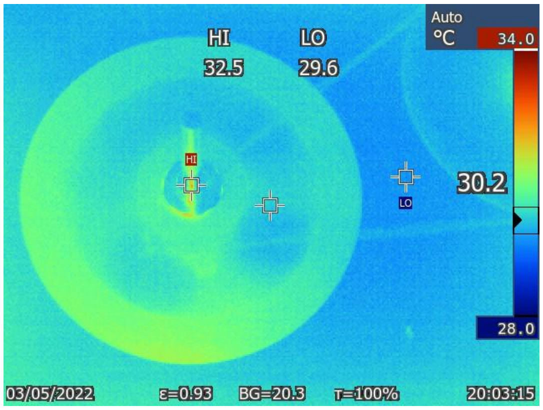	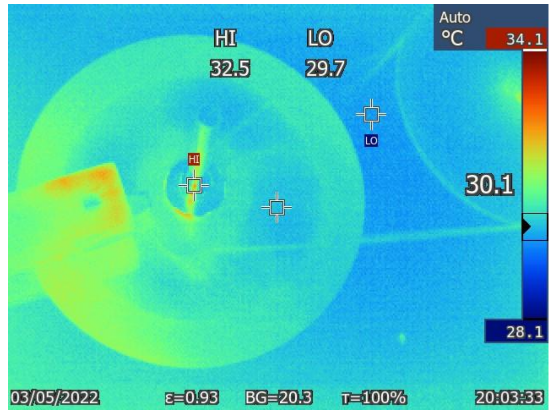

16-Hole Disk

Trial	Before Magnets	After Magnets
1	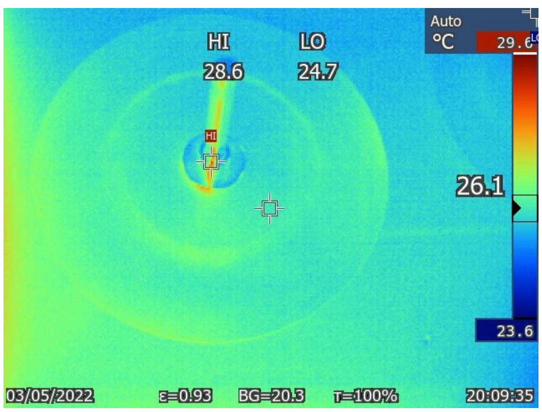	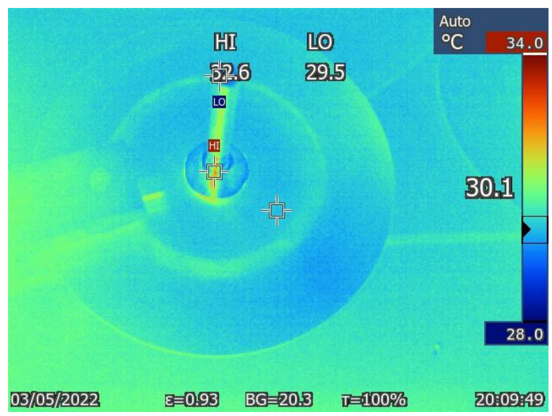
2	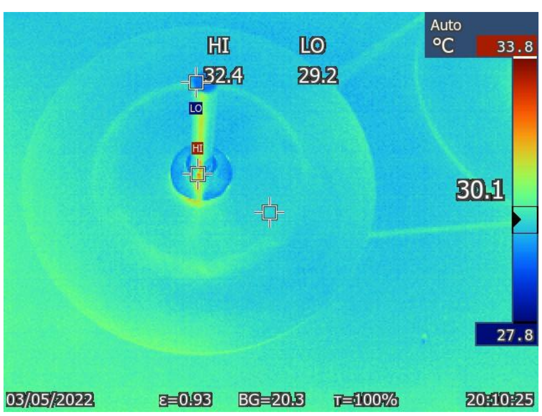	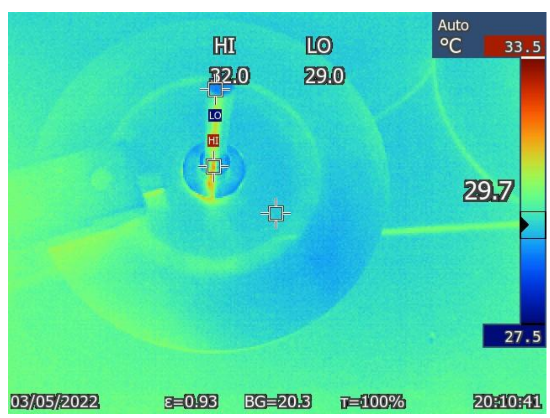

<table>
<tr><td>3</td><td>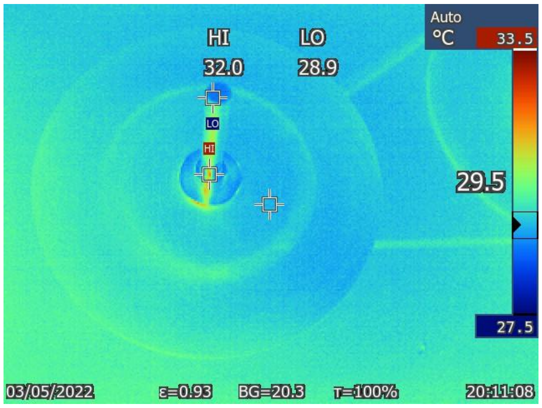
</td><td>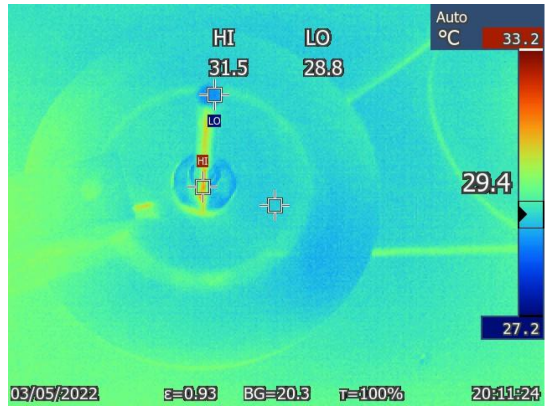
</td></tr>
<tr><td>4</td><td>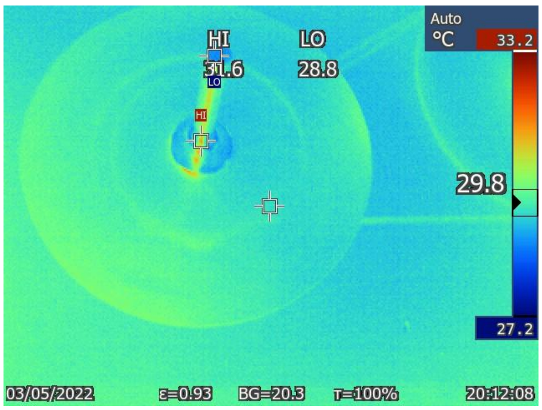
</td><td>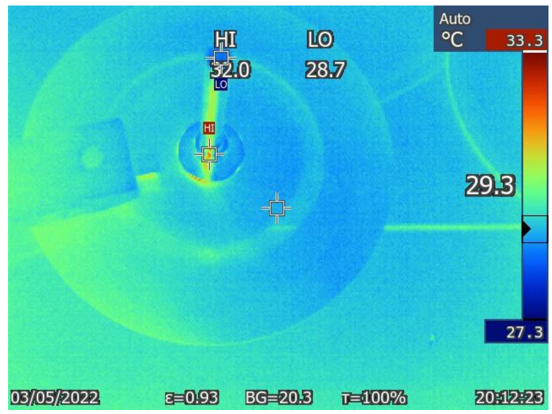
</td></tr>
<tr><td>5</td><td>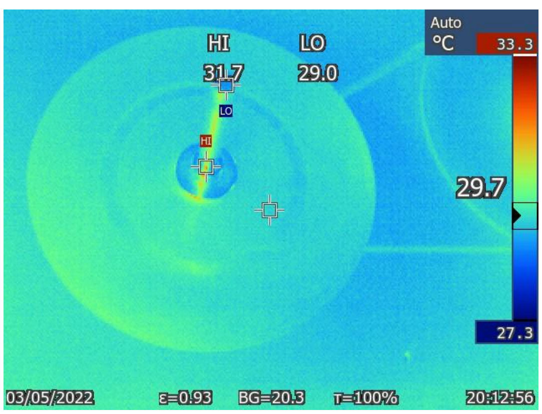
</td><td>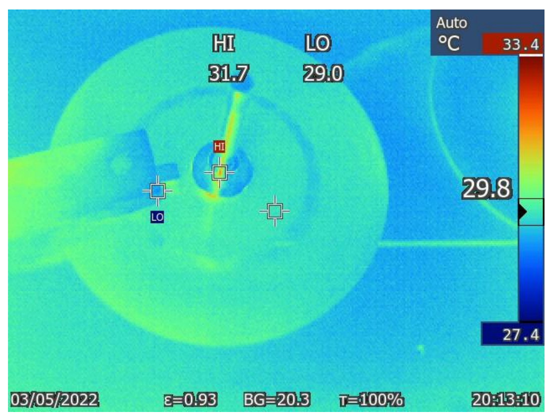
</td></tr>
</table>

Appendix C: Project Milestones

Milestone 1

One document (pdf) with a numbered list of candidate research project topics. Phrase these as a question that would be answered by the research by the end of the term.

1. What effect do elevated heart rate and a higher body temperature have on focus or fine motor control?
2. Game-related motion, ex ping pong, etc. Does the angle of the arm affect the acceleration of the ball thrown?
3. Does the shortening of the time of cooking tasks reduce the probability of grip loss?
    a. Tracking grip fatigue
    b. Mimicking the task flow of a worker (i.e. a cook) and tracking the fatigue in their dominant hand.
4. How much does muscle temperature impact its function?
5. Is there an optimal tacking angle for sailboats based on wind speed?
    a. Tough to test; requires a significant setup (scale sailboat, wind tunnel, small pool of water) – a lot of variables to isolate
6. What are the limitations of common sensors? That is, when does data get wonky?
    a. For instance, how much strain is too much strain? Or how hot or cold can a thermosensor operate?

Summarize the main points of your discussion with your team about any concerns or planning ideas.

- We are concerned that we are only doing ideas that relate to the human body, which could be due to what we have read thus far from other projects. Therefore, we believe there might be more interesting/diverse ideas that evolve later and could very much be better than these listed.
- Another concern can be how strong or tough the sensors are for them to return correct data under relatively extreme conditions. For example, measuring heart rate during running can be difficult and under heavy risk of failure.
- There are budget concerns for some of the ideas.
- There might not be enough time to properly measure, analyze, plot, and interpret our data if we take too long choosing a project.

Milestone 2

Candidate Research Questions:

1. How does temperature affect the effectiveness of eddy currents in electromagnetic braking systems?
    a. Theoretical Foundations: Thermal analysis, eddy currents (general conductors), eddy currents (copper pipe), eddy current breaking in automobiles, magnetic transformation of mechanical energy to thermal energy, material resistivity's dependence on temperature, Lenz's Law,

    Summary:
    - Eddy currents are electric currents that have been generated within a conductor by a magnetic field. Because these currents cannot flow anywhere, they swirl and dissipate heat. Lenz's law allows us to determine the direction of electric current and is what can be used to hypothesize the flowment of the eddy current.
    - Our magnetic field will come from an electromagnet and using Lenz's law, which states that "the direction of the electric current induced in a conductor by a changing magnetic field is such that the magnetic field created by the induced current opposes changes in the initial magnetic field", we conclude that an induced eddy current will generate a magnetic field on the non-ferrous disk. If we make the motor constantly power the disk to rotate at a constant speed, an opposing electromotive force will be created and slow down the disk, with heat being generated on the disk as a by-product. Therefore, we will be testing various holes or the lack of holes on 3 different disks in order to see the effect of change in eddy currents on the effectiveness of the braking system.

2. Is 3D printed geometry better than traditionally made material in terms of sound cancellation?
    a. Theoretical Foundations: Sound is a type of wave that spreads in media. When it spreads in air, its intensity typically becomes smaller when distance between the source and the receiver gets longer, and it possesses properties of reflection, refraction, and diffraction when encountering a solid surface. Reflection is when a sound wave bounces in certain angles from the surface, refraction is when the wave's trajectory is distorted by the change in the media (density, moisture, etc.), and diffraction is that the wave can still transfer after hitting a small obstacle by moving around it (the object's dimension should be smaller than the wavelength of the wave). Besides these properties, a sound wave can also be absorbed by obstacles. As the wave travels deeper into the material, its energy is removed and intensity becomes smaller, just like its reduction in the air. When a wave hits a solid surface, absorption and reflection happen at the same time (Sound Absorption). Therefore, it is reasonable to speculate that a product with the right

material and geometry will absorb, reflect and trap audible sound waves to an extent that they are virtually inaudible.

b. Metamaterials allow one to change the wave propagation of sound. Therefore, metamaterials are able to be manipulated in order to control audible sound waves. The study of material composition and design are at the core of this experiment. Additionally, in the field of acoustics, metamaterials have the function of changing the direction of sound. This is possible when you create a metamaterial that has a refractive index, a measure of the speed of wave passing through a material, that is negative or zero. Metamaterials are nuanced things because they are different from what can be found in nature. Materials that are found in nature all have a K (Bulk Modulus) that is greater than zero. This is not ideal when wanting to control sound waves because that means that those materials dampen acoustic energy when sound waves hit them.
Source (controlling sound with acoustic metamaterial):

3. Does there exist a relationship between the amount of friction the vehicle experiences while driving and the vehicle's ability to correct its error?
    a. Theoretical Foundations:
        i. Closed-loop control is a method to monitor and adjust a system's state based upon how the system changes under environmental influences. A common type of controller used in managing vehicle motion is a PID controller, which corrects system error by summing the error function with its derivative and integral at some time *t* and multiplying each by specific gain constants that are inherent in the system. This error sum is then added to the next instance of the system to try to make the system error smaller than it was previously.
        Source (https://en.wikipedia.org/wiki/PID_controller)
        ii. Road friction is a function of many variables, including road surface, tire surface, weather, and speed. All of these do change in the duration of a single drive, so the question stands if control gains need to be adjusted during a drive to account for the change in road friction or if there exist optimal gain values that can be universally applied to the controller function, regardless of road condition.
        Source (https://intblog.onspot.com/driving-dynamics-what-is-road-friction)

Consultant Concerns

1. Temperature and Magnetic Field: (C&P from Odin's slack message↓)
Professor Chiesa:
"Hi Odin,

This is an interesting question and unfortunately I do not have experience on this (particularly magnetic brakes).
I am happy to discuss this further but here's some resources that might be useful to start.

https://www.explainthatstuff.com/eddy-current-brakes.html
https://youtu.be/2PqWmBUEk5k
https://www.comsol.com/blogs/how-eddy-current-braking-technology-is-freeing-us-from-friction/"

Professor Chiesa, while an expert in superconductors which have a primary function of performing as electromagnets, was not experienced with electromagnetic braking specifically. She did, however, provide helpful resources for us to visualize how eddy-current brakes work and the effect they have on temperature.

A follow up was required, so the team met over zoom with Professor Huang. The following are notes from the meeting to develop our idea into a testable concept:

- Disk magnetic brakes have holes => eddy currents more effective with holes?
- Impact of holes on cooling surface temperature, can it be incorporate without reduction of magnetic flux/braking => expect to affect magnetism and cooling
- Literature review and it will be fruitful for application with great variety in design
- Look into 'magnetic hysteresis' and related effects
- Practically: Construct metal disk on bearing, create magnetic field w mockup bench top experiment. Shoot for rough data showing that you are either affecting cooling or magnetic field.
- Test same setup and two different speed changes for disk 1 vs 2 (varying design)
- Try a solid disk, a disk with few big holes, a disk with many small holes but the same area missing.
- Plan out for how air comes in and air leaves (constantly refreshing air flow) .
- Would be difficult to visualize/measure magnetic field; otherwise embedded thermocouple within disk to check temperature distribution OR infrared gun to measure temperature for non-contact
- How to simulate rotational accelerate, constant speed, motor power cutout, momentum afterwards
- Need to machine and assemble robotic devices => expect to troubleshoot
- Figure out the simplest way to put a motor on a disk and spin up to target speed, and build the magnetic brake as a totally separate part to control
- Run trials and collect sample data to understand braking action; if no different, gather any results and find supportive evidences (empirical or analytical) to support the trend (even if there's no trend)

2. <u>Sound Resistance of 3D Printed Geometries:</u>

Notes taken during meeting with Professor Huang (Zoom meeting):
2/18/2021

- Be careful about the typical application; this is not a design course
- You want to investigate the shape of the microphone cones because we wanted to prove that this shape is best for sound amplification
- We want to end with a report that creates information for future designers, not a design that we created
- Noise cancellation: Your speaker isn't the same as the source of noise, you are sending waves as much as you are canceling them. It would be difficult to create a new idea
- What about ideas for the structure of the material to better cancel noise? The vibration theory says that in structural damping, vibration comes in, the whole structure can eliminate damping
    - It has to be a Christmas tree structure of different designs
    - How do you 3D print different structures for noise cancellation? Our motivation is that we don't have to build a complex structure. We can investigate a different shape that we hypothesize what shape would be best because of these features
    - Investigate what structures are best
    - Maybe a tiny structure would be great at eliminating vibration (Prof. White's research)
    - Some related research for what
- 3D printed with the same number of fins
- Something that was cone shaped so it could resonate with different frequencies
- We put different sensors or a high-speed camera to see whether they were vibrating at different frequencies
- What questions could we ask because we have better 3D printing?
- Let's start talking to a consultant (Rob White) because we don't know if this question is feasible or reasonable

Madeline spoke to professor Professor Robert White on Zoom

Overall Feedback: This project has been done many times before. We would need to change something very specific in order to make this work according to the criteria of the ME 70 Project requirements. Prof. White offered to let us borrow equipment and informed us that many of the parts we need are very cheap. He led us to find out more about Metamaterials. We chose not to do this because this has been done so much. There are even companies encouraging people to 3D print metamaterials such as Sculpteo.

3. Driving Friction in relation to Correctable Error:

Summary of Professor Huang's concerns (zoom meeting):

The original question was warned to be more about simulation and experimental validation. During our zoom meeting with Professor Huang, possible alternatives that used similar theories were also discussed. One of these was the examination of a control problem that would require the usage of a simulation-like a robotic car.

- Simulation heavy
- Is there a theory
- How to change to make it a good question? Did we get stuck here? And thats why we decided to give up?
- Would also spend most of our time working on simulation, coding, creating robot and not on instruments, experimentation, and theory exploration.

The meeting concluded that this would not be a feasible project, so we did not attempt to continue with the theory, and to focus on our better prospects.

Bibliography

Andersson, Ulrik. "Driving Dynamics – What Is Road Friction?" The Onspot Blog – International, https://intblog.onspot.com/driving-dynamics-what-is-road-friction.

Bansal, Miyu, and John Duivestein. "The Effect of Temperature on the Braking Force Experienced by Magnet Falling through a Copper Pipe." *Journal of Student Research*, vol. 10, no. 2, 2021, https://doi.org/10.47611/jsrhs.v10i2.1503.

(Basel, Switzerland), MDPI, 30 Apr. 2019, https://www.ncbi.nlm.nih.gov/pmc/articles/PMC6539407/.

Chris Woodford. Last updated: March 23. "How Do Eddy-Current Brakes Work?" *Explain That Stuff*, 23 Mar. 2021, https://www.explainthatstuff.com/eddy-current-brakes.html.

Cook, J. G., et al. *Thermal and Electrical Conductivity of Aluminum.* . 1 Sept. 1975, https://www.osti.gov/servlets/purl/5066461.

Cummer, Steven A., et al. "Controlling Sound with Acoustic Metamaterials." *Nature Reviews Materials*, vol. 1, no. 3, 2016, https://doi.org/10.1038/natrevmats.2016.1.

"How Eddy Current Braking Technology Is Freeing Us from Friction." *COMSOL*, https://www.comsol.com/blogs/how-eddy-current-braking-technology-is-freeing-us-from-friction/.

"Lenz's Law." *Wikipedia*, Wikimedia Foundation, 28 Feb. 2022, https://en.wikipedia.org/wiki/Lenz%27s_law#:~:text=Lenz%27s%20law%2C%20named%20after%20the,in%20the%20initial%20magnetic%20field.

Ma, Der-Ming, and Jaw-Kuen Shiau. "The Design of Eddy-Current Magnet Brakes." *Transactions of the Canadian Society for Mechanical Engineering*, vol. 35, no. 1, 2011, pp. 19–37., https://doi.org/10.1139/tcsme-2011-0002.

Magcraft. "What Are Eddy Currents?" *MAGCRAFT Brand Rare Earth Magnets*, 30 Apr. 2015, https://www.magcraft.com/blog/what-are-eddy-currents#:~:text=The%20magnetic%20field%20produced%20by,eddy%20currents%20is%20magnetic%20levitation.

Monzón-Verona, José Miguel, et al. "Thermal Analysis of a Magnetic Brake Using Infrared Techniques and 3D Cell Method with a New Convective Constitutive Matrix." *Sensors*

Nath, Sarath G, et al. "Eddy Current Braking in Automobiles." *International Research Journal of Engineering and Technology*, 4 Apr. 2018.

"Pid Controller." Wikipedia, Wikimedia Foundation, 22 Feb. 2022, https://en.wikipedia.org/wiki/PID_controller.

"Sound Absorption." *Sound Absorption - an Overview | ScienceDirect Topics*, https://www.sciencedirect.com/topics/engineering/sound-absorption.

Milestone 3

Statement of Explanation

As part of any braking system for moving vehicles, a circular disk mounted to the wheel is designed so a damping force applied to the disk will eventually cause the wheel to decelerate and come to a full stop. The efficiency of brakes determines how quickly a moving object can be stopped to avoid long deceleration distance and ensure the passenger's safety when an emergency situation is recognized.

The most commonly used braking mechanism called "disk brake", often seen in cars and bicycles, utilizes the friction force caused by a pair of pads squeezing onto the disk to slow the shaft rotation. Our group is set to explore another braking mechanism that utilizes electromagnetism to slow down the mounted disk: eddy current brakes. In real-life application, these brakes are used for subways, trains, and airplanes. Therefore, electromagnetic brakes are much less common and highly proprietary, leading to research not being published. We aim to simulate and provide the testing results of eddy current brakes to the general public, as we believe it's very much important for the end-users to be aware and validate their safety of these under-explored systems.

Theory & Hypothesis

A non-ferrous disk moves through the magnetic field created by the brake/electromagnets will create an induced current on the disk. Because the disk is constantly rotating, the magnetic field is also created with the magnetic flux over a given area of the disk increasing as it gets closer to the brakes/electromagnets. Through Faraday's law of induction, the changing magnetic flux creates an electric field and current onto the conductive, non-ferrous disk. This induced current found on the brake disk is called Eddy Current.

At this moment, the initial magnetic field is caused by electromagnets. With Lenz's law, which states that "the direction of the electric current induced in a conductor by a changing magnetic field is such that the magnetic field created by the induced current opposes changes in the initial magnetic field", we conclude that the induced Eddy Current will generate a magnetic field on the non-ferrous disk. Since the motor is still constantly powering the disk to rotate at a constant speed, an opposing electromotive force will be created and slow down the braking disk, with heat being generated on the disk as a by-product.

Given the widely-accepted notion of "lower temperature associated with a stronger magnetic field, and higher temperature associated with a weaker temperature", our group hypothesizes that the distribution of holes on a braking disk can improve the efficiency of the braking system. While this design theoretically would interrupt the Eddy Currents' interaction with the disk, we reason that the heat dissipated by the distribution of holes would outweigh the less contact time. In other words, our hypothesis is that using the braking disk with more holes would result in a somewhat-less effective braking system, but the system will be more efficient overall by remaining at a manageable temperature to keep the disk's magnetic properties intact.

Experimental Plan

To model the braking disk mounted on a high-speed rotational axle of a heavyweight vehicle, our tentative setup is as follows: a scale-down circular disk powered by a high-torque motor along with two strong electromagnets on both sides.

The material for the circular disk must be non-ferrous metal so it would not be attracted to the operating electromagnets but still has to be conductive. Given the material availability at Bray, thin sheets of aluminum are an obvious choice: light-weight, ease of fabrication, and low cost compared to the steel variation found in actual eddy current brakes.

Aluminum disks of the same inertia will vary in the number of holes; One disk will have smaller and more plentiful holes and the other disk bigger but with fewer holes. Thus the removed mass from the disks will not change. We are ultimately trying to see which disk design leads to a faster decrease in velocity and is a better braking system.

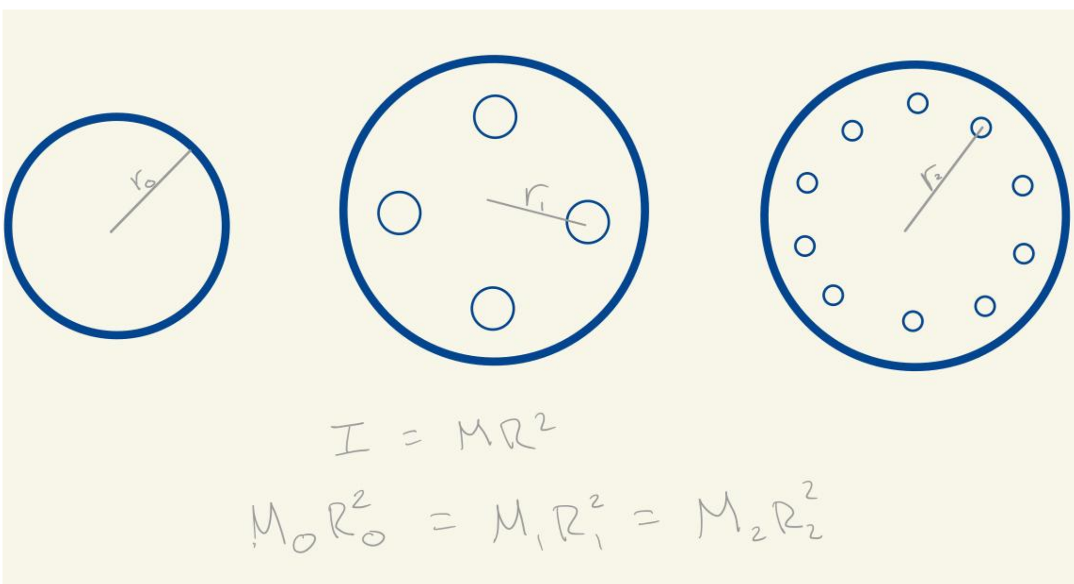

Visual of 3 disks. Disk 0 will be our control. Not to scale and the # of holes is not accurate, this is just a rough visual representation.

Data will be collected by taking three brake disk designs and spinning them to a constant angular speed in multiple trials. The first design will be a solid circular disk. The second disk will have six holes cut at a specified radius, and have a total radius slightly larger than the first. The third disk will have 24 holes cut out at the same specified radius and will add up to the mass of the holes removed from the second disk. The third disk will also have a slightly larger radius than the first. This will create three disks with the same moment of inertia, but different designs to study.

With the disks spun up to speed (with the motor's angular velocity measured by an encoder), a magnet will be applied at the radius of the holes for all three disks. An IR thermometer will measure the effect the different hole designs have on the disk's temperature rise. A timer will be used from the time the magnet is applied to the time the disk comes to a halt. We can plot the disk temperatures (maximum) versus the deceleration time and run statistical tests to determine if a relationship exists. This data will allow for the analysis of multiple points of interest. The first being the overall effect the hole designs have on deceleration. Further correlations might also exist between temperature and hole design and temperature and deceleration.

Materials

<u>Borrowed</u>	<u>Ordered</u>
IR Thermometer (Bray Equipment Room)	Aluminum Disks (Bray Machine Shop)
L298N H Bridge (from group member)	Stepper Motor (+ encoder) https://www.omc-stepperonline.com/stepper-motor-w-encoder/nema-23-closed-loop-stepper-motor-3nm-425oz-in-with-magnetic-encoder-1000ppr-4000cpr-23hs45-4204-me1k
Arduino Nano (from group member)	Magnet https://www.adafruit.com/product/3873

Bill of Materials for Ordering:
https://docs.google.com/spreadsheets/d/17SaGuvCW0BwV-a25vhuuFfIUkY2VDX0sOUzEzZOYyho/edit?usp=sharing

Milestone 4

Hardware

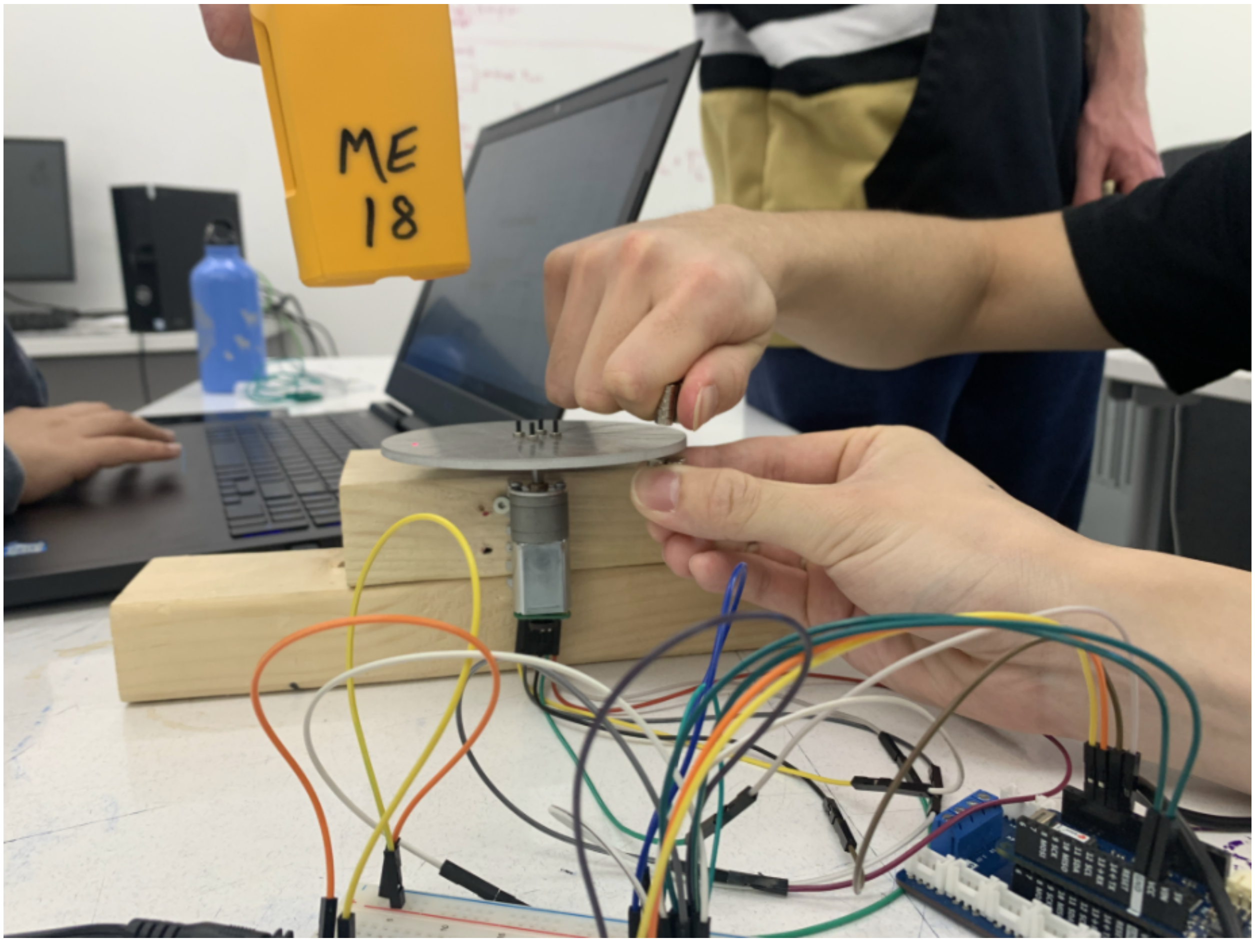

Our prototype setup

For our prototype, we had a 10cm diameter aluminum disk cut by Bray staff that we fixed to a motor assembly from the ME031 labs. The motor was driven by an H-Bridge and Arduino MKR, which ran the code attached at the end of this document. To mimic a magnetic brake, two group members held permanent magnets close to the spinning disk (but not touching it). While the motor ran, the program collected position and speed data about the disk**,** both with and without the magnets influencing it. We also borrowed an IR gun from Bray that we used to measure the surface temperature of the disk, to see if the magnets successfully transformed some of the disk's kinetic energy into thermal energy. However, the gun's accuracy is very questionable, considering that it recorded a group member's skin's surface temperature to be over 50℃. We will look into substituting the IR gun for a thermal imaging chip that we can mount close to the disk to resolve the temperature accuracy concern.

Video of Prototype

https://tufts.app.box.com/file/930485569656

Sample Plots

The following plots were constructed by a MATLAB program that measured the angular position, angular velocity, and raw encoder counts of the motor and disk assembly both with and without magnetic interference.

Angular Position

With Magnets

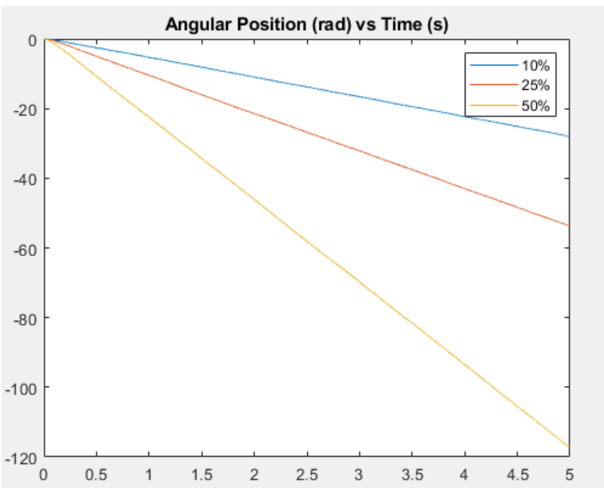

Without Magnets

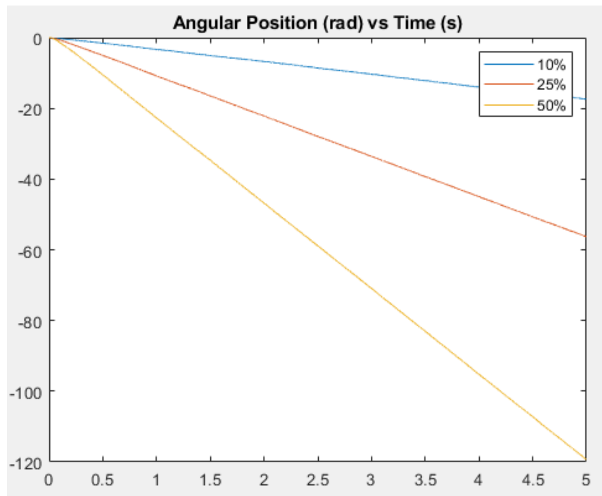

Angular Velocity

With Magnets

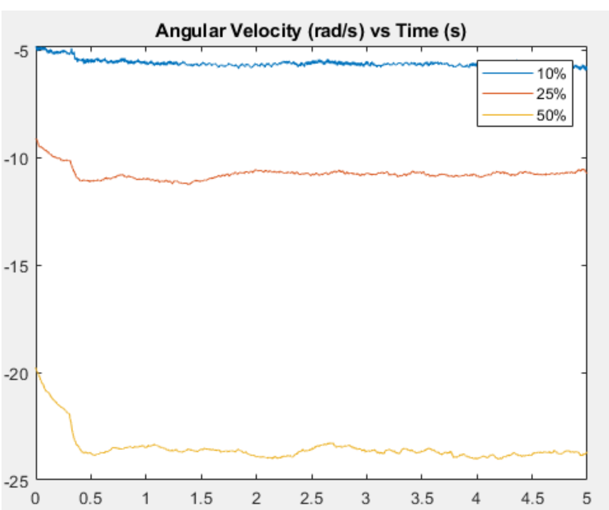

Without Magnets

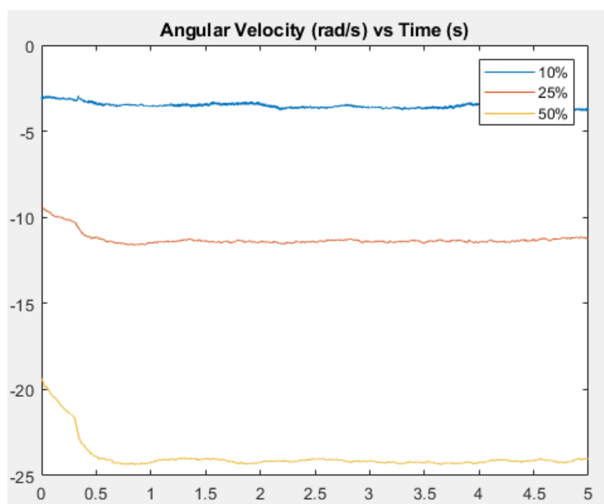

Encoder Counts

With Magnets

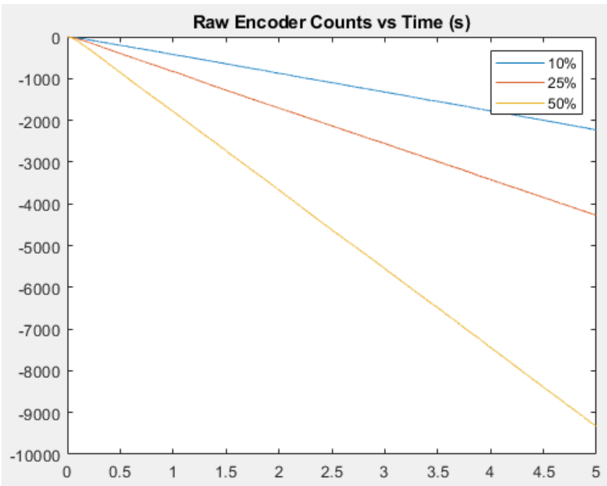

Without Magnets

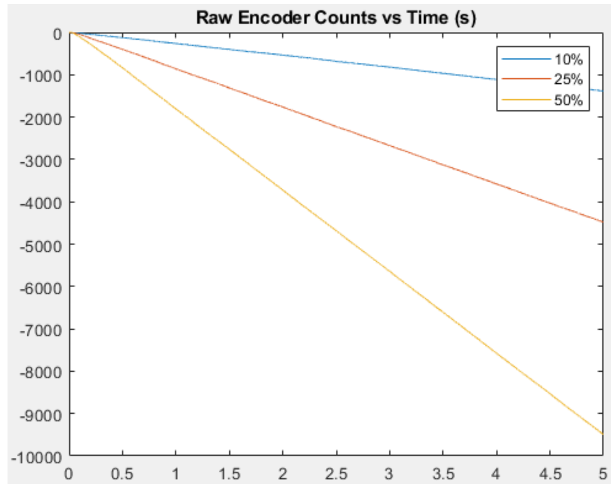

Code

```
% ME070 Milestone 4 - Prototype


% To test drive the motor, use myArduino.PWMDrive(1,0.2); where the first

% parameter refers to Motor 1, and the second parameter refers to the PWM

% duty cycle (-1 = 100% backwards, 0 for stop, 1 for 100% forward)


% WIRING NOTE:

% M2 needs to be connected to H Bridge's INA to get positive drive

%


clc

clear

close all


myArduino = ME31arduino('COM7');
```

```
% ======================
% MEASURING STEP RESPONSE
% ======================
PWM_level = [0.10; 0.25; 0.50];
stepResponse = [];
for i = 1:3
    myArduino.ResetEncoder();

    % 1 : PWM1 (Motor #1) is the drive, Encoder 1 is the measurement
    myArduino.SetHighSpeedMode(1);

    % Will record 4096 datapoints, dt is calculated as (total time)/(4096)
    dt = 5/4096;                    % this will run for 3 seconds in total
    myArduino.SetTimeStep(dt);

    % STEPVOLTAGE is the largest step that your microcontroller unit can output
    % (in this case with the MKR its 3.3) Modify this value by any factor of n
    % (where 0 < n < 1) to obtain n*100 % PWN level drive
    myArduino.GetStepResponse(3.3 * PWM_level(i))
    stepResponse = [stepResponse, myArduino.data];
            pause(1);
end


% ======================
% PROCESSING DATA
% ======================
x = myArduino.t;
```

```
y = myArduino.data;
figure(1)
plot(myArduino.t, stepResponse)
title('Raw Encoder Counts vs Time (s)')
legend('10%', '25%', '50%')

theta = stepResponse .* ((2*pi)/500); %% counts -> revolutions -> radians
figure(2)
plot(myArduino.t, theta)
title('Angular Position (rad) vs Time (s)')
legend('10%', '25%', '50%')

for i = 1:3
        omega = gradient(theta(:,i), myArduino.dt);
        omega_fil = movmean(omega, 500);
        figure(3)
        plot(myArduino.t, omega_fil)
  hold on
end
title('Angular Velocity (rad/s) vs Time (s)')
legend('10%', '25%', '50%')
```

Milestone 5

Video of the system running with the encoder reading shaft position:
https://drive.google.com/file/d/1f59UdNcnQE22QTAmKc1w2kLMvCjWq9UU/view?usp=sharing

Arduino Code to run the motor:

```
// Define pins
int driverPUL = 7;    // PUL- pin
int driverDIR = 6;    // DIR- pin
// Define PWM width and initial direction
int pd = 250;       // Pulse Delay period, controls speed of motor–longer period, slower motor
//boolean setdir = LOW; // Set Direction
void setup() {
        pinMode (driverPUL, OUTPUT);
        pinMode (driverDIR, OUTPUT);
}
// Run pulse HIGH and LOW once each to create a 50% duty cycle (percentage recommended by
// the motor driver)
void loop() {
        //digitalWrite(driverDIR,LOW);
        digitalWrite(driverPUL,HIGH);
        delayMicroseconds(pd);
        digitalWrite(driverPUL,LOW);
        delayMicroseconds(pd);
}
```

LabVIEW Code to manage the encoder and plot the raw encoder counts:

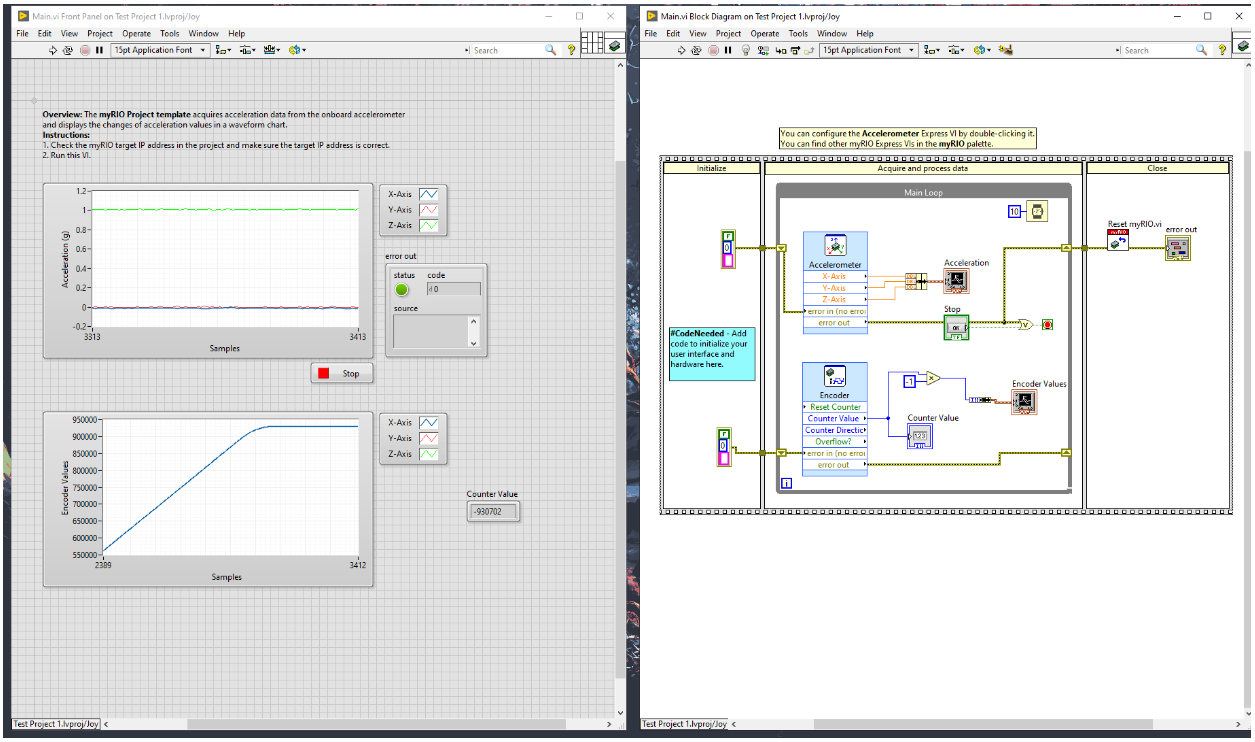

Appendix D: Data Process Code

```
% ME70 Final Project Analysis

% Raw Data Importation  (Commented out once run once)
for import = 1
% C1 = xlsread('control_trial1.xlsx',-1); % Trial 1 Control
% C2 = xlsread('control_trial2.xlsx',-1);
% C3 = xlsread('control_trial3.xlsx',-1);
% C4 = xlsread('control_trial4.xlsx',-1);
% C5 = xlsread('control_trial5.xlsx',-1);
%
% F1 = xlsread('marcel_trial1.xlsx',-1); % Trial 1 Four Hole Disk
% F2 = xlsread('marcel_trial2.xlsx',-1);
% F3 = xlsread('marcel_trial3.xlsx',-1);
% F4 = xlsread('marcel_trial4.xlsx',-1);
% F5 = xlsread('marcel_trial5.xlsx',-1);
%
% S1 = xlsread('dariel_trial1.xlsx',-1); % Trial 1 Sixteen Hole Disk
% S2 = xlsread('dariel_trial2.xlsx',-1);
% S3 = xlsread('dariel_trial3.xlsx',-1);
% S4 = xlsread('dariel_trial4.xlsx',-1);
% S5 = xlsread('dariel_trial5.xlsx',-1);
end

for d = 1
C1sam = C1(:,1);
C1spe = C1(:,5);
C2sam = C2(:,1);
C2spe = C2(:,5);
C3sam = C3(:,1);
C3spe = C3(:,5);
C4sam = C4(:,1);
C4spe = C4(:,5);
C5sam = C5(:,1);
C5spe = C5(:,5);

F1sam = F1(:,1);
F1spe = F1(:,5);
F2sam = F2(:,1);
F2spe = F2(:,5);
F3sam = F3(:,1);
F3spe = F3(:,5);
F4sam = F4(:,1);
F4spe = F4(:,5);
F5sam = F5(:,1);
F5spe = F5(:,5);

S1sam = S1(:,1);
S1spe = S1(:,5);
S2sam = S2(:,1);
S2spe = S2(:,5);
S3sam = S3(:,1);
S3spe = S3(:,5);
S4sam = S4(:,1);
S4spe = S4(:,5);
S5sam = S5(:,1);
S5spe = S5(:,5);

end

% Raw Data Disp.
% Control
for c= 1
figure(1)
```

```
tiledlayout(5,1)
nexttile
plot(C1sam, C1(:,5))
title('Control Disk (Raw Trials)')
ylabel('Angular Speed (rev/s)')
nexttile
plot(C2sam, C2(:,5))
ylabel('Angular Speed (rev/s)')
nexttile
plot(C3sam, C3(:,5))
ylabel('Angular Speed (rev/s)')
nexttile
plot(C4sam, C4(:,5))
ylabel('Angular Speed (rev/s)')
nexttile
plot(C5sam, C5(:,5))
ylabel('Angular Speed (rev/s)')
xlabel('Sample Number')

end

% Four Hole Disk
for f =1
figure(2)
tiledlayout(5,1)
nexttile
plot(F1sam, F1(:,5))
title('Four Hole Disk (Raw Trials)')
ylabel('Angular Speed (rev/s)')
nexttile
plot(F2sam, F2(:,5))
ylabel('Angular Speed (rev/s)')
nexttile
plot(F3sam, F3(:,5))
ylabel('Angular Speed (rev/s)')
nexttile
plot(F4sam, F4(:,5))
ylabel('Angular Speed (rev/s)')
nexttile
plot(F5sam, F5(:,5))
ylabel('Angular Speed (rev/s)')
xlabel('Sample Number')

end

% Sixteen Hole Disk
for s =1
figure(3)
tiledlayout(5,1)
nexttile
plot(S1sam, S1(:,5))
title('Sixteen Hole Disk (Raw Trials)')
ylabel('Angular Speed (rev/s)')
nexttile
plot(S2sam, S2(:,5))
ylabel('Angular Speed (rev/s)')
nexttile
plot(S3sam, S3(:,5))
ylabel('Angular Speed (rev/s)')
nexttile
plot(S4sam, S4(:,5))
ylabel('Angular Speed (rev/s)')
nexttile
plot(S5sam, S5(:,5))
ylabel('Angular Speed (rev/s)')
```

```
xlabel('Sample Number')

end



% Filtration of Data
[B,A] = butter(2, .02)

for filt = 1
C1filt = filtfilt(B,A,C1spe);
figure(4)
plot(C1sam(1:length(C1filt)),C1filt)
C2filt = filtfilt(B,A,C2spe);
hold on
plot(C1sam(1:length(C2filt)),C2filt)
C3filt = filtfilt(B,A,C3spe);
plot(C1sam(1:length(C3filt)),C3filt)
C4filt = filtfilt(B,A,C4spe);
plot(C1sam(1:length(C4filt)),C4filt)
C5filt = filtfilt(B,A,C5spe);
plot(C1sam(1:length(C5filt)),C5filt)
title('Filtered Control Disk Speed vs. Encoder Count')
xlabel('Encoder Count')
ylabel('Revolutions per Second')



F1filt = filtfilt(B,A,F1spe);
figure(5)
plot(F1sam(1:length(F1filt)),F1filt)
hold on
F2filt = filtfilt(B,A,F2spe);
plot(F1sam(1:length(F2filt)),F2filt)
F3filt = filtfilt(B,A,F3spe);
plot(F1sam(1:length(F3filt)),F3filt)
F4filt = filtfilt(B,A,F4spe);
plot(F1sam(1:length(F4filt)),F4filt)
F5filt = filtfilt(B,A,F5spe);
plot(F1sam(1:length(F5filt)),F5filt)
title('Four Hole Disk Disk Speed vs. Encoder Count')
xlabel('Encoder Count')
ylabel('Revolutions per Second')


S1filt = filtfilt(B,A,S1spe);
figure(6)
plot(S1sam(1:length(S1filt)),S1filt)
hold on
S2filt = filtfilt(B,A,S2spe);
plot(S1sam(1:length(S2filt)),S2filt)
S3filt = filtfilt(B,A,S3spe);
plot(S1sam(1:length(S3filt)),S3filt)
S4filt = filtfilt(B,A,S4spe);
plot(S1sam(1:length(S4filt)),S4filt)
S5filt = filtfilt(B,A,S5spe);
plot(S1sam(1:length(S5filt)),S5filt)
title('Sixteen Hole Disk Speed vs. Revolution')
xlabel('Encoder Count')
ylabel('Revolutions per Second')

end
```

```
% Trim to start of braking
for Ctrim = 1
   figure(10)
Ctrimx = linspace(0,length(C1sam(310:end)),length(C1sam(310:end)));
C1trimy = C1filt(310:end);
plot(Ctrimx, C1trimy);
hold on
C2trimy = C2filt(176:175+length(Ctrimx));
plot(Ctrimx, C2trimy);
hold on
C3trimy = C3filt(225:224+length(Ctrimx));
plot(Ctrimx, C3trimy);
hold on
C4trimy = C4filt(190:189+length(Ctrimx));
plot(Ctrimx, C4trimy);
hold on
C5trimy = C5filt(250:249+length(Ctrimx));
plot(Ctrimx, C5trimy);
hold on
title('Trimmed and Filtered Control Disk')
ylabel('Angular Speed (rev/sec)')
xlabel('Sample Number')
end

for Ftrim = 1
   figure(11)
Ftrimx = linspace(0,length(F3sam(259:end)),length(F3sam(259:end)));
F1trimy = F1filt(248:247+length(Ftrimx));
plot(Ftrimx, F1trimy);
hold on
F2trimy = F2filt(245:244+length(Ftrimx));
plot(Ftrimx, F2trimy);
hold on
F3trimy = F3filt(259:258+length(Ftrimx));
plot(Ftrimx, F3trimy);
hold on
F4trimy = F4filt(107:106+length(Ftrimx));
plot(Ftrimx, F4trimy);
hold on
F5trimy = F5filt(177:176+length(Ftrimx));
plot(Ftrimx, F5trimy);
hold on
title('Trimmed and Filtered Four Hole Disk')
ylabel('Angular Speed (rev/sec)')
xlabel('Sample Number')
end

for Strim = 1
   figure(12)
Strimx = linspace(0,length(S4sam(218:end)),length(S4sam(218:end)));
S1trimy = S1filt(136:135+length(Strimx));
plot(Strimx, S1trimy);
hold on
S2trimy = S2filt(160:159+length(Strimx));
plot(Strimx, S2trimy);
hold on
S3trimy = S3filt(172:171+length(Strimx));
plot(Strimx, S3trimy);
hold on
S4trimy = S4filt(218:217+length(Strimx));
plot(Strimx, S4trimy);
hold on
S5trimy = S5filt(112:111+length(Strimx));
plot(Strimx, S5trimy);
hold on
```

```
title('Trimmed and Filtered Sixteen Hole Disk')
ylabel('Angular Speed (rev/sec)')
xlabel('Sample Number')
end


%%% Split Analysis %%%

for all_analysis =1
for initiate = 1
Cxvec = (cat(2, Ctrimx,Ctrimx,Ctrimx,Ctrimx,Ctrimx));
Cyvec = rot90(cat(1, C1trimy, C2trimy, C3trimy, C4trimy, C5trimy));
Fxvec = (cat(2, Ftrimx,Ftrimx,Ftrimx,Ftrimx,Ftrimx));
Fyvec = rot90(cat(1, F1trimy, F2trimy, F3trimy, F4trimy, F5trimy));
Sxvec = (cat(2, Strimx,Strimx,Strimx,Strimx,Strimx));
Syvec = rot90(cat(1, S1trimy, S2trimy, S3trimy, S4trimy, S5trimy));

end
%Steady State Analysis
for steady =1
   % C is steady 300-700
   % F is steady 300-750
   % S is steady 300-750
Cxsteady = (cat(2, Ctrimx(300:700),Ctrimx(300:700),Ctrimx(300:700),Ctrimx(300:700),Ctrimx(300:700)));
Cysteady = rot90(cat(1, C1trimy(300:700), C2trimy(300:700), C3trimy(300:700), C4trimy(300:700), C5trimy(300:700)));
Cysteady_arr = [C1trimy(300:700), C2trimy(300:700), C3trimy(300:700), C4trimy(300:700), C5trimy(300:700)];
Fxsteady = (cat(2, Ftrimx(300:750),Ftrimx(300:750),Ftrimx(300:750),Ftrimx(300:750),Ftrimx(300:750)));
Fysteady = rot90(cat(1, F1trimy(300:750), F2trimy(300:750), F3trimy(300:750), F4trimy(300:750), F5trimy(300:750)));
Fysteady_arr = [F1trimy(300:750), F2trimy(300:750), F3trimy(300:750), F4trimy(300:750), F5trimy(300:750)];
Sxsteady = (cat(2, Strimx(300:750),Strimx(300:750),Strimx(300:750),Strimx(300:750),Strimx(300:750)));
Systeady = rot90(cat(1, S1trimy(300:750), S2trimy(300:750), S3trimy(300:750), S4trimy(300:750), S5trimy(300:750)));
Systeady_arr = [S1trimy(300:750), S2trimy(300:750), S3trimy(300:750), S4trimy(300:750), S5trimy(300:750)];

figure(19)
scatter(Cxsteady,Cysteady, 'k')
hold on
scatter(Fxsteady,Fysteady, 'r')
hold on
scatter(Sxsteady,Systeady, 'b')
title('Steady State Speed vs. Time')
xlabel('Encoder Sample')
ylabel('Speed (rev/sec)')
end
%Slope Analysis
for slope =1
   % C is sloping 0-200
   % F is sloping 0-200
   % S is sloping 0-200
Cx_d_slope = (cat(2, Ctrimx(1:200),Ctrimx(1:200),Ctrimx(1:200),Ctrimx(1:200),Ctrimx(1:200)));
Cy_d_slope = rot90(cat(1, diff(C1trimy(1:200)), diff(C2trimy(1:200)), diff(C3trimy(1:200)), diff(C4trimy(1:200)), diff(C5trimy(1:200))));
Cy_d_slope_arr = [diff(C1trimy(1:200)), diff(C2trimy(1:200)), diff(C3trimy(1:200)), diff(C4trimy(1:200)), diff(C5trimy(1:200))];
Fx_d_slope = (cat(2, Ftrimx(1:200),Ftrimx(1:200),Ftrimx(1:200),Ftrimx(1:200),Ftrimx(1:200)));
Fy_d_slope = rot90(cat(1, diff(F1trimy(1:200)), diff(F2trimy(1:200)), diff(F3trimy(1:200)), diff(F4trimy(1:200)), diff(F5trimy(1:200))));
Fy_d_slope_arr = [diff(F1trimy(1:200)), diff(F2trimy(1:200)), diff(F3trimy(1:200)), diff(F4trimy(1:200)), diff(F5trimy(1:200))];
Sx_d_slope = (cat(2, Strimx(1:200),Strimx(1:200),Strimx(1:200),Strimx(1:200),Strimx(1:200)));
Sy_d_slope = rot90(cat(1, diff(S1trimy(1:200)), diff(S2trimy(1:200)), diff(S3trimy(1:200)), diff(S4trimy(1:200)), diff(S5trimy(1:200))));
Sy_d_slope_arr = [diff(S1trimy(1:200)), diff(S2trimy(1:200)), diff(S3trimy(1:200)), diff(S4trimy(1:200)), diff(S5trimy(1:200))];
figure(20)
scatter(Cx_d_slope(1:length(Cy_d_slope)),Cy_d_slope, 'k')
hold on
scatter(Fx_d_slope(1:length(Fy_d_slope)),Fy_d_slope, 'r')
hold on
scatter(Sx_d_slope(1:length(Sy_d_slope)),Sy_d_slope, 'b')
title('Acceleration Vs. Time for Each Trial')
xlabel('Encoder Sample')
```

```
ylabel('Acceleration (rev/sec/sample)')
end
for ttest=1
    for steady = 1
        Css = [mean(Cysteady_arr)];
        Fss = [mean(Fysteady_arr)];
        Sss = [mean(Systeady_arr)];

    end
    for slope = 1
        Cslope = [mean(Cy_d_slope_arr)];
        Fslope = [mean(Fy_d_slope_arr)];
        Sslope = [mean(Sy_d_slope_arr)];

    end
end
end

%figure(30)
%scatter(Cxvec,Cyvec);
%Cconfin = confidenceIntervalPlot(Cxvec,Cyvec);
```